Standardization Procedure to Provide a Unified Multi-Method Elemental Compositional Dataset, Application to Ferruginous Colouring Matters from Namibia

Guilhem Mauran, Benoit Caron, Lucile Beck, Florent Détroit, Camille Noûs, Olivier Tombret, David Pleurdeau, Jean-Jacques Bahain, Matthieu Lebon

Standardization procedure to provide a unified multi-method elemental compositional dataset, application to ferruginous colouring matters from Namibia

AUTHORS

Guilhem MAURAN[a, b] (https://orcid.org/0000-0002-3884-5194),

Benoit CARON[c] (https://orcid.org/0000-0001-7051-4339),

Lucile BECK[d],

Florent DéTROIT[a] (https://orcid.org/0000-0001-5208-6203),

Camille NOÛS[e,1], (https://orcid.org/0000-0002-0778-8115),

Olivier TOMBRET[a],

David PLEURDEAU[a],

Jean-Jacques BAHAIN[a] (https://orcid.org/0000-0002-1446-5568),

Matthieu LEBON[a] (https://orcid.org/0000-0003-4970-1230)

[a]*UMR 7194 Histoire Naturelle de l'Homme Préhistorique (HNHP), Museum national d'Histoire naturelle - CNRS -UPVD, Association Sorbonne Universités, Musée de l'Homme, 17 Place du Trocadéro, 75116 Paris, France*

[b]*Evolutionary Studies Institute (ESI), University of the Witwatersrand, PO Wits 2050, Johannesburg, South Africa*

[c]*UMR 7193 Institut des Sciences de la Terre de Paris (ISTeP), Sorbonne Université, CNRS-INSU, F-75005 Paris, France*

[d]*Laboratoire de Mesure du Carbone 14 (LMC14), LSCE/IPSL, CEA-CNRS-UVSQ, Universite Paris-Saclay, F-91191 Gif-sur-Yvette, France*

[e]*Cogitamus* Laboratory, 1 ¾ rue Descartes, 75005 Paris, France

Corresponding author: Guilhem MAURAN: guilhem.mauran1@edu.mnhn.fr, 0027647075419, 1 Jan Smuts Avenue, Braamfontein 2000, Johannesburg, South Africa

[1] *Camille Noûs embodies the collegial nature of our work, as a reminder that science proceeds from* disputatio *and that the building and dissemination of knowledge are intrinsically selfless, collaborative and open.*

ABSTRACT

Curation of archaeological materials often leads to carrying out multi-analytical methodologies that combine non-invasive and invasive elemental analyses. Such materials are often analysed with different techniques. It results in the production of complementary but apparently non-compatible compositional datasets that cannot be easily compared. In the present paper, we propose to compare results acquired on geological ferruginous colouring matters from Namibia with analytical techniques (X-Ray Fluorescence spectrometry (XRF), Proton-Induced-X-ray Emission spectrometry (PIXE), Inductively Coupled Plasma coupled to Optical Emission spectrometry (ICP-OES) and Inductively Coupled Plasma coupled to Mass Spectrometry (ICP-MS)). We aim to provide a unified elemental dataset about these ferruginous colouring matters, usually referred to as “ochre” in archaeology. Analysed geological samples come from three distinct tectonostratigraphic zones of Namibia surveyed in the frame of rock art research. When compared directly, three of the four datasets obtained from these measurements appear as non-compatible because of the inter-equipment variability. However, through a simple standardization procedure, we demonstrate that it is possible to unify these datasets. This procedure minimizes the inter-equipment variability, making the inter-zones of provenance predominant and allowing distinctions of the samples according to their sole origin. Beyond shedding new light on the possibility to compare different elemental analytical techniques, this procedure paves the way for robust statistical provenance studies of ferruginous colouring matter.

KEYWORDS

Compositional data; Standardization; multi-method; Ferruginous colouring matter; Namibia

1.INTRODUCTION

Ferruginous colouring matters correspond to a wide variety of rocks rich in iron-oxides which can transmit their colour to another material. Most archaeologists refer to them under the "ochre" catch-them-all term (Onoratini, 1985; Dayet, 2012; Chalmin et al., 2021; Salomon et al., 2021; Popelka-Filcoff and Zipkin, 2022).These colouring matters occur in different archaeological contexts such as mine and open-air site, rock shelter or cave. Within these contexts, they are present in various forms: as small boulders and fragments in the archaeological assemblage, as residues over tools or beads or as pigments used for rock art. These remains record numerous information concerning past communities cognition, behaviours, techniques and mobility (d'Errico, 2003 ; Salomon et al., 2012 ; Hodgskiss, 2014; Mathis et al., 2014 ; Lebon et al., 2019 ; Dayet, 2021; Domingo and Chieli, 2021; Huntley, 2021; Popelka-Filcoff and Zipkin, 2022). The observation and characterization of these materials allow the description of the succession of mental steps and technical gestures aimed at exploiting, processing, and using these materials. This succession of steps is referred to as "*chaîne opératoire*" (Perles, 1987: 23). Here, it becomes possible to investigate the methods of preparation of these resources (Wadley, 2005a, Hodgskiss, 2010), the choice made by the populations in the type of colouring matter they exploited(Mathis et al., 2014), their different use of these raw materials (Wadley, 2005a,b, Rifkin, 2015 ; Rifkin et al., 2015) , as well as the mobility of these past communities (Mauran et al., 2021a ; Huntlet, 2021 ; Velliky et al., 2021).

During the last two decades, advances in analytical instrumentation have led to an increase in the number of studies about archaeological ferruginous colouring matters. These advances implied the use of different elemental analytical techniques to characterize the materials and determine the provenance of the archaeological ferruginous colouring matters: X-Ray Fluorescence spectrometry (XRF) (Jercher et al., 1998 ; Lebon et al., 2019) , particle-induced X-ray emission (PIXE) (Erlandsen et al. 1999; Bernatchez et al. 2008 ; Nel et al., 2010 ; Beck et al., 2011. 2012 ; Salomon et al., 2012 ; Mathis et al., 2014 ; Lebon et al., 2014) , instrumental neutron activation analysis (NAA) (Kiehn et al., 2007 ; Popelka-Filcoff et al., 2007, 2008 ; Eiselt et al., 2011 ; MacDonald et al., 2013, 2018 ; Velliky et al., 2021) , inductive coupled plasma – optical emission spectrometry and mass spectrometry (ICP-OES and ICP-MS) coupled or not to laser ablation (Green an Watling, 2007 ; Iriarte et al., 2009 ; Dayet et al., 2013 ; Scadding et al., 2015 ; Moyo et al., 2016 ; Zipkin et al., 2017, 2020 ; Eiselt et al., 2019 ; Pierce et al., 2020 ; Mauran et al., 2021a) . An extensive review of these studies has been recently published by Dayet (2021).

The aforementioned techniques present different advantages and disadvantages regarding their analytical specificities: destructiveness, analytical costs, range of measured elements at once, repeatability and accessibility (Fig. 1). There is a clear demand for instruments with high repeatability and accuracy but also economical, widely accessible and of minimal invasiveness for preserving these

unique archaeological artefacts. Not all these requirements can be met altogether, often leading researchers to downscale their studies and repeat analyses of the same sample with different analytical techniques. The selection of one of these techniques is material, context, and problem dependant (Salomon et al., 2016 ; Zipkin et al., 2020 ; Dayet, 2021) . The development of multi-technical approaches, combining non-invasive and invasive analyses allow accessing all different aspect of past exploitations of ferruginous colouring matter (Dayet , 2012 ; Chalmin and Huntley, 2018 ; Mauran, 2019 ; Domingo and Chieli, 2021).

When one tries to study the whole "*chaîne opératoire*" of these ferruginous resources, the absolute necessity of their preservation leads to carrying out multi-analytical methodologies that combine non-invasive and invasive analyses. On one side, using ICP-OES/ICP-MS on geological samples would provide an accurate fingerprint of the potential sources, but result in destroying the samples, which can't be done for most of archaeological assemblages On the other side, using non-destructive but less sensitive analyses such as air-extracted microbeam PIXE and pXRF for highly valued archaeological samples and residues would allow their preservation while providing limited information about their potential provenance (Fig. 1) (Mauran, 2019).

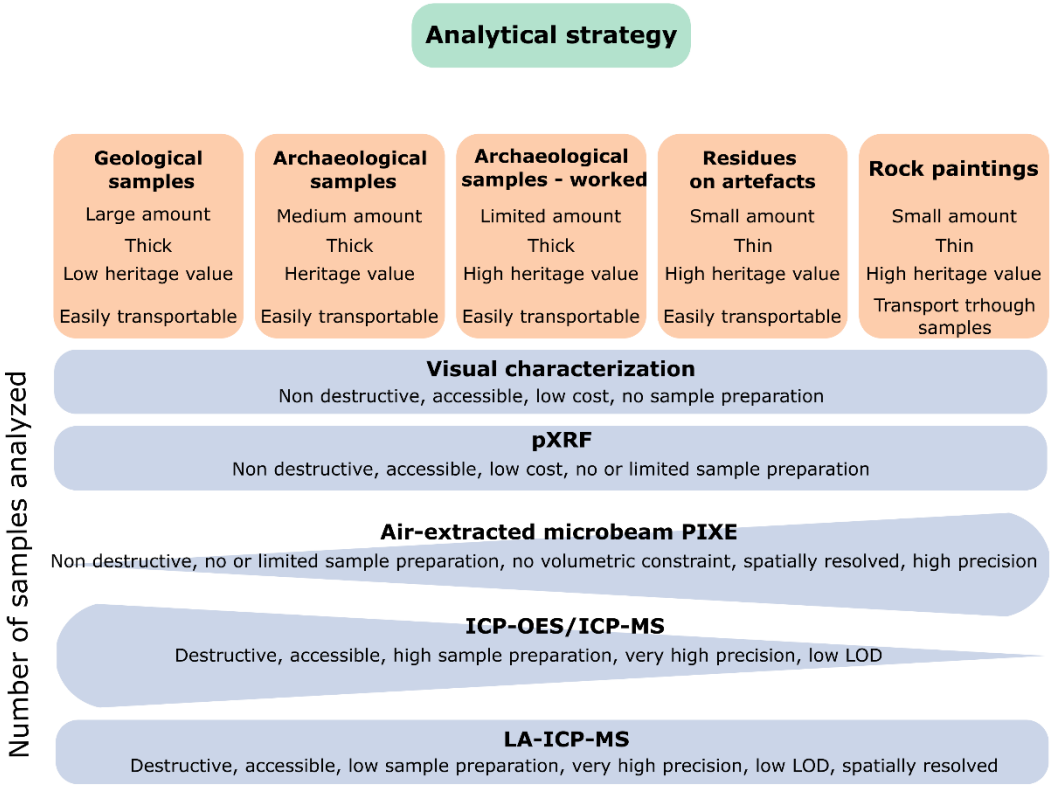

Fig. 1. Ideal analytical strategy to investigate the geochemical composition of ferruginous colouring matter. (double columns, colour)

The use of these techniques with different sensitivity and precision produces complementary but non-compatible compositional datasets. However, between-laboratory variations can limit comparisons of datasets acquired from distinct instruments or even on different days (Yellin et al., 1978 ; Popelka-Filcoff et al., 2012 ; Salomon et al., 2016) Fundamental differences in experimental conditions between distinct techniques raise more difficulties (Hein et al., 2002 ; Tsolakidou et al., 2002 ; Glascock et al., 2004) . So far, this has prevented researchers to reuse and share compositional data of ferruginous colouring matter acquired with different techniques or at distinct laboratories thus restricting studies to answer punctual questions (Salomon et al., 2016 ; Chanteraud et al., 2021). Previous works attempted to compare data acquired on ferruginous colouring matter samples with different techniques (SEM-EDS, PIXE, ICP-OES) (Dayet, 2012, 2021). Dayet mainly investigated the accuracy of these techniques and highlighted the influence of patina on geochemical data. Works performed by Salomon and colleagues (2016) shed light on the importance of using standards to compare data. Popelka-Filcoff and colleagues (2012), compared NAA measures acquired at two different facilities. They concluded to the equivalence of the datasets but the impossibility to combine them directly. Research aiming to compare data acquired by different analytical methods have been carried out on other materials such as ceramics, glaze, and obsidians (Hein et al., 2002 ; Grave et al., 2005 ; Speakman et al., 2011 ; Mitchell et al., 2012 ; Kasztovszky et al., 2018). However, all these works only compared the techniques and their efficiency to discriminate the provenance origins of different raw material. Inter-equipment calibrations remain scarce, one of the most successful projects is the CHARM project. During this project, Heginbotham and colleagues (2015) have developed XRF inter-laboratory standardization for copper alloys characterization. Maximum Fe_2O_3 content in these alloys is of 1.4 ± 0.9 % (32X SN5A) (Heginbotham et al., 2015 ; Steenstra et al., 2021). Ferruginous colouring materials usually have a Fe_2O_3 content comprised between 10 to 90 %. This difference of composition prevents the direct use of this inter-laboratory calibration for colouring materials characterization. Elemental analyses provide large datasets usually containing more than ten elemental concentrations (variables) and often a higher number of samples (observations). Questions answered with these elemental analyses usually consist in 1) discriminating groups of artefacts according to their elemental composition (categorisation), 2) comparing the artefacts elemental composition with modern raw material elemental composition (sourcing). Answering these questions involves investigating the structure of the elemental datasets. To do so, researchers often use exploratory multivariate analyses. Among the most often used multivariate analyses are principal component analysis (PCA) and linear discriminant analysis (LDA). Both analyses are presented in detail for ochre studies by Zipkin and colleagues (2017), and iron slags by Leroy (2010) or more generally by Baxter (1994) .

Principal component analysis (PCA) is most of the time used as an unsupervised method.... PCA allows reduction of the number of variables and mainly maximises the variability over the whole dataset. Linear discriminant analysis (LDA) is a supervised method that also allows reducing the number of variables

but maximises the ratio of between-class variance to within-class variance. In this sense, LDA is more susceptible to discriminate groups than PCA, due to the inherent structure provided to perform the analysis. In this sense, PCA allows the investigation of the structure of the datasets while LDA allows better discrimination of distinct groups.

PCA, the most common method used in colouring matter provenance, is a scale dependant analysis. Therefore, variables with the highest intensity weigh more than others in the statistical analysis. When investigating datasets with concentrations expressed in different units such as percentages and parts per million, data treatments are a necessity to ensure an equal weight to all the variables. This is why data are usually transformed. Numerous transformations exist to tackle this issue. Data standardization to zero mean and unit variance or log-ratio transformations are however the most common, sometimes used together (Baxter, 1995).

The use and advantages of standardization and log-transformation have been debated elsewhere (MacDonald et al., 2013, 2018 ; Zipkin et al., 2017, 2020 ; Mauran et al., 2021a) . The most common method for colouring matter provenance studies relies on the Fe- normalization methodology (e.g. David et al., 1993 ; Smith et al., 1998 ; Popelka-Filcoff et al., 2007). After a statistical correlation test such as Pearson's is performed, only elements correlated with Fe are used in subsequent analyses. Considerations about elements correlation are further discussed in the literature (e.g. Popelka-Filcoff et al., 2007; Beck et al., 2011; Mathis et al., 2014; Lebon et al., 2018; MacDonald et al. 2011; Dayet et al., 2016; Dayet, 2021). These elements are then normalized to the iron content. These ratios are then log-transformed. But recent studies have highlighted some of the limits of this method (Dayet et al., 2016 ; MacDonald et al., 2018, Pierce et al., 2020) Other transformations such as direct logarithm or centred-log-ratio transformations have been successfully developed (Zipkin et al., 2017 ; Pierce et al., 2020; Mauran et al., 2021a) . The centred-log-ratio transformation is a more general transformation than the Fe-log-ratio one, for which elemental concentrations are normalized to the geometrical mean of the concentrations of all elements considered. According to Aitchison (1982), this transformation is more robust than the Fe-log-ratio transformation to sub-composition (a subset composition) use.

Since 2015, we investigate the use of ferruginous colouring matters at the Later Stone Age site of Leopard Cave (Erongo, Namibia) (Mauran et al., 2020, 2021a,b). A large part of the colouring matters recovered at the site are massive haematites. We already proved the possibility to provenance Namibian ferruginous colouring matter with invasive ICP-OES/ICP-MS technique (Mauran et l., 2021a) . But such a procedure is only possible for geological and few unmodified archaeological blocks leaving aside most of the archaeological artefacts. Therefore, most of the "*chaîne opératoire*" remains difficult to investigate. As we aim to study the whole "*chaîne opératoire*" of ferruginous colouring matter processing, we investigated the possibility to compare compositional data acquired with different analytical techniques. We hope to combine their advantages as presented in figure 1.

In this paper, we apply multivariate analysis on datasets obtained on colouring materials from central Namibia by X-Ray Fluorescence spectrometry (XRF), Proton-Induced-X-ray Emission spectrometry (PIXE), Inductively Coupled Plasma coupled to Optical Emission spectrometry (ICP-OES) and Inductively Coupled Plasma coupled to Mass Spectrometry (ICP-MS). We aim to unify these different compositional datasets of ferruginous colouring matters to provide the possibility to study the whole "*chaînes opératoires*" and have a better understanding of past populations behaviours and mobility. Our results are relevant beyond the scope of ferruginous colouring materials as they can provide a way to go for multimodal inter laboratory comparisons of artefacts of high cultural heritage importance, which cannot be analysed destructively.

2.MATERIAL AND METHODS

2.a. Material

Ferruginous colouring matters analysed in this study are geological samples. We collected them at seven outcrops in three distinct tectonostratigraphic zones around Leopard Cave in north-central Namibia (Mauran et al., 2021a, b). These three zones are the North Zone (NZ), the igneous Kalkfeld Complex (Kalkfeld), and the Central Zone (CZ) (Fig. 2). They respectively correspond to what we previously considered as regional provenance, sub-local provenance and local provenance areas (Mauran et al., 2021a). Our initial archaeological question focused on the existence of raw material circulation between different Namibian rock art massif. Each of the massif falls into different tectonostratigraphic zone (Mauran et al., 2021a). This is why, we grouped different localities into groups corresponding to the tectonostratigraphic zones. All samples were collected in 2017 and exported in agreement with permit ES 31957 granted to G.M. Table 1 sums up the origin and the analyses performed on each sample. 52 samples were analysed by XRF, 23 by PIXE and 55 by-both-ICP-OES and ICP-MS by a same operator with the help of specialists of each analytical method. Samples from Kalkeld zone correspond to igneous hematite-magnetite ore and ferruginous breccia form from their alteration. Samples from the North Zone correspond to hematite -goethite nodules of volcanic and igneous origin and hematite sandstone resulting from their alteration. Samples from the Central Zone are ferruginous hematite-goethite nodules come from lens of possible igneous origin.

Standards BXN (bauxite), DRN (diorite), IFG (iron formation) from SARM Laboratory (CRPG Nancy) and 11 samples were analysed with all four methods: ICP-OES, ICP-MS, PIXe and pXRF (Table 2). Among these 11 samples, four came from Kalkfeld complex, 4 from Central Zone and 3 from North Zone.

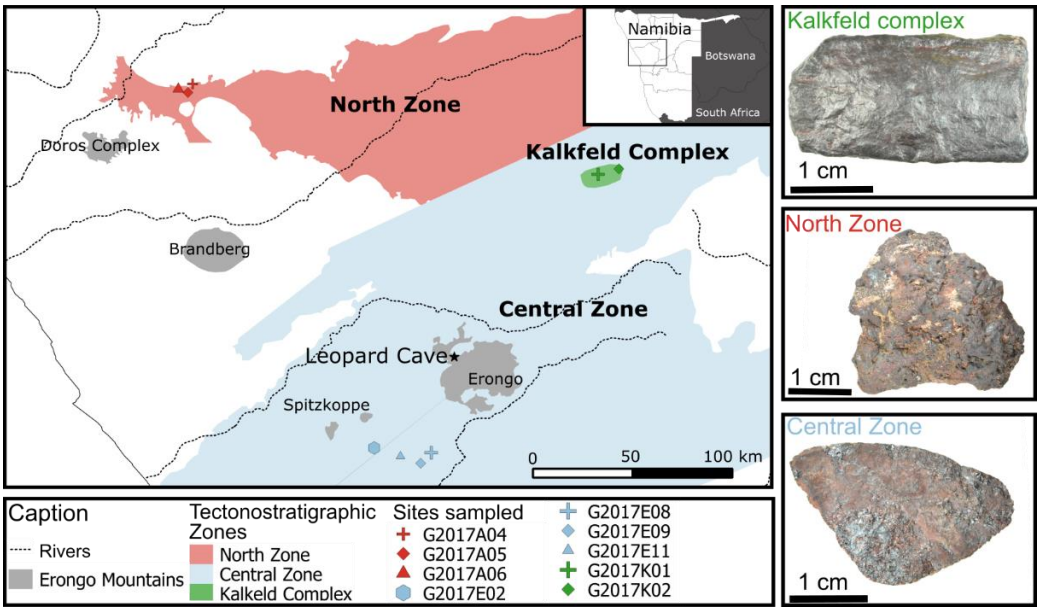

Figure 2. Geological context (left) and selected examples (right) of the Namibian geological samples analysed in the study. (double column, colour)

Table 1. List of outcrops from which samples were analysed in this study with mention of their tectonostratigraphic zone of origin.

Outcrop	Zone	Number of samples analysed by ICP	Number of samples analysed by PIXE	Number of samples analysed by pXRF
G2017K01	Kalkfeld Complex	3	2	5
G2017K02	Kalkfeld Complex	6	2	5
Total Kalkfeld Complex		9	4	10
G2017E02	Central Zone	10	3	5
G2017E08	Central Zone	7	4	7
G2017E09	Central Zone	5	0	5
G2017E11	Central Zone	7	4	6
Total Central Zone		29	8	23
G2017A04	North Zone	5	2	5
G2017A05	North Zone	5	2	7
G2017A06	North Zone	8	4	7
Total North Zone		18	8	19
Total		56	23	52

2.b. XRF analysis

X-ray fluorescence spectrometry (XRF) analyses were carried out at the Musée de l'Homme, MNHN, Paris, France using an Elio portable X-Ray fluorescence spectrometer developed by XGLAB (Bruker). This system is composed of an X-ray source based on an Rh anode. The anode operates at a voltage between 10 and 40 kV and a current up to 200 µA for maximal power of 4 W. Detection is ensured by a Silicon Drift Detector with an active area of 25 mm^2. The emitted beam source is collimated to a spot diameter of 1.2 mm on the sample at a working distance of 1.4 cm. Analyses were performed at 40 kV and 100 µA, with an accumulation time of 300 s. Spectra were treated using PyMca software to calculate elemental concentrations from fundamental parameters (Solé et al., 2007). Usually, this fundamental parameters approach does not require a standard calibration. To validate our approach, we measured three standards: BXN, DRN and IFG. All these samples were prepared as pressed powders. As pXRF has relatively high LOD for minor and trace elements for ferruginous materials, LOD were estimated and values below LOD were subjected to zero-substitution (see Data treatment). For pXRF analyses, samples were analysed as is. Most samples presented "fresh" break with no patina. Samples weight between 3 to 80g. Raw pXRF results are presented in Electronic Supplementary Information (ESI) 1.

2.c. PIXE analysis

Proton-induced X-ray Emission spectrometry analyses have been carried out with the external proton beam of NEW-AGLAE (C2RMF, Louvres Museum, Paris, France) (Pichon et al., 2015 ; Lebon et al., 2018) . Before analysis, samples were sawed to obtain a plan of analyses inside each sample with minimal influence of the outside patina or any surface contamination. The cut samples were then analysed with no further preparation. Measurements were performed using 3 MeV protons beam with a diameter of around 40 µm on samples. Large areas (at least 2 x 2 mm) were scanned thanks to horizontal/vertical mechanical movements to average samples composition. Time acquisition, around 3 min, was adjusted according to a dose rate detector to obtain an identical dose on each sample.

Low and high energy X-Ray emissions were recorded using Peltier-cooled SDD detectors (50 mm^2). One detector was devoted to low energies (Mg to Fe) and three to high energies (Fe and above). Two high energy detectors were covered by a 20 µm thick chromium and a 50 µm thick aluminium filter. The third high energy detector was covered by a 150 µm thick aluminium filter. These filters reduce pileup effects and the X-rays induced by the Cr filter (Swann et al., 1990 ; Beck et al., 2012) . Fe quantification was used as a pivot between the low and high energies (Beck et al., 2011). The selected experimental conditions are similar to previous PIXE ferruginous colouring matters analyses carried out at AGLAE (Beck et al., 2011, 2012 ; Lebon et al., 2018). In such conditions, the detection limits are between 10 and more than 100 ppm according to the element. Spectra treatment and elemental quantification were performed using TRAUPIXE and GUPIX software (Pichon et al., 2010). The

GUPIX software relies on the use of a configuration file that allows spectrum modelling considering the specificities of each experiment. The configuration file used was optimised by measurement performed on the DRN (diorite, 70% aluminosilicate) standard, used to compare PIXE day to day quantifications. All three standards BXN, DRN and IFG were prepared as pressed powders. Raw PIXE results are presented in ESI 2.

2.d. ICP-OES and ICP-MS analysis

Elemental characterization of each sample was performed using both solutions Inductively Coupled Plasma Optical Emission Spectroscopy (ICP-OES) and Inductively Coupled Plasma Mass Spectrometry (ICP-MS) at the ALIPP6 Platform (Sorbonne Université, ISTeP). 100 mg of homogenized powder (50 mg for ICP-OES and 50 mg for ICP-MS) were digested in acidic solutions and then analyzed according to the protocol of the ALIPP6 and published by Mauran and colleagues (Mauran et al., 2021a). In addition to standards BXN, DRN, IFG, ICP-OES and ICP-MS were calibrated thanks to the following reference materials: FeR-1 (Iron formation), FeR-2 (Iron formation), FeR-3 (Iron formation), FeR-4 (Iron formation), ATHO-G (rhyolitic glass), BHVO-2 (basalt), BCR-1 (basalt), BIR-1 (basalt), GSN, and RGM-1(rhyolite) (ESI 3). All these standards were prepared according to the same protocol than the samples. Raw ICP-OES and ICP-MS results are presented in ESI 4 and on the online open access repository (Mauran et al., 2021b – http://doi.org/10.5281/zenodo.3908304).

ICP-OES analyses were carried out on a 5100 SVDV Agilent ICP-OES and allowed us to quantify the following 21 chemical elements: Si, Al, Mg, Na, K, Ti, Fe, Mn, Ca, P, Sr, Ba, Sc, V, Cr, Zr, S, W, Cu, Zn, Co. For each of these elements, between two and four wavelengths were measured over an exposure time of 3 times 20 s.

ICP-MS analyses were carried out on a 8800 Agilent ICP-MS/MS and allowed us to quantify the following 37 chemical elements: ^{7}Li, ^{45}Sc, ^{51}V – ^{53}V, ^{52}Cr, ^{59}Co, ^{60}Ni, ^{63}Cu, ^{66}Zn, ^{71}Ga, ^{75}As, ^{85}Rb, ^{88}Sr, ^{89}Y, ^{90}Zr, ^{93}Nb, ^{95}Mo, ^{133}Cs, ^{137}Ba, ^{139}La, ^{140}Ce, ^{141}Pr, ^{146}Nd, ^{147}Sm, ^{153}Eu, ^{157}Gd, ^{159}Tb, ^{163}Dy, ^{165}Ho, ^{166}Er, ^{169}Tm, ^{172}Yb, ^{175}Lu, ^{178}Hf, ^{181}Ta, ^{206}Pb – ^{207}Pb – ^{208}Pb, ^{232}Th, ^{238}U .

Our comparison of elements concentration quantified by ICP-OES and ICP-MS (V, Cr, Co, Cu, Zn, Sr, Zr, Ba, Sc) demonstrated that the two techniques are complementary (Mauran et al., 2021a). The ICP-OES analyses allow the quantification of major, minor and few trace elements, while ICP-MS ones provide quantification of a large range of trace elements. To avoid elements redundancy between the ICP-OES and ICP-MS measures, we arbitrary decided to use for subsequent analyses the ICP-MS values for these elements (Mauran et al., 2021a).

2.e. Data treatment

Zero Value substitution. Common data treatment for ferruginous colouring matters data statistical analyses rely on the use of logarithm (e.g. David et al., 1993 ; Popelka-Filcoff et al., 2007, 2008). One issue of the use of logarithm is the existence of zero values. Zero values could correspond to a real absence, called "essential" zero, or to the presence of an element in smaller quantities than the limit of detection (LOD), called "rounded" zero. Because these "rounded" zero are different than the "essential" zero it seems reasonable to replace them. In compositional studies, several approaches exist to replace these zero values. Two large families of substation procedure exist: Simple substitutions or advanced substations procedures. Simple substitutions rely on replacing the rounded zero for a constant positive value smaller than the limit of detection of the analytical technique used to perform the measurement (Palarea-Albaladejo et al. 2014). As such simple approach risks biasing the datasets more advanced substitution have been developed (Aitchison, 1986 ; Baxter, 1994 ; Martín-Fernández et al. 2003 ; Palarea-Albaladejo and Martin-Fernandez 2013). These advanced methods attempt to preserve the ratio relationship among the variables (or in our case element) thanks to closure procedure. However, closing the data to 100 % can induce false elemental correlation and that only the ratio between the elements is of interest for compositional data analyses (Aitchison, 1982). In ochre studies, rounded zero substitution has been discussed by Zipkin et al., (2020)

As we decided to avoid closure procedures for the reasons mentioned above, in the current study, we decided to perform a "simple substitution". Before applying logarithm transformation, concentrations below the limits of detection of the considered technique were substituted by a value of 10% of the minimal value.

Standardization procedures. To unify the obtained datasets, two different standardization procedures were tested in the present study. The two procedures only differ in the way we performed the merger and standardization of the dataset obtained from the different analytical technique. Both standardization procedures relied on the following formula:

$$x_{ij} = \frac{C_{ij} - \bar{C_i}}{\sigma C_i} \quad (1)$$

where x_{ij} is the standardized concentration of an element I for a sample j, C_{ij} the concentration of an element i for a sample j, $\bar{C_i}$ the mean concentration of element i in all samples, and σC_i the standard deviation of element i concentration.

The first procedure referred to post merged standardization consisted in applying formula (1) on the merged datasets without any consideration of the analytical techniques providing the measure. The dataset obtained from this first procedure is called the post merged dataset (ESI 5).

The second standardization procedure consisted in applying formula (1) on each dataset separately before merging the datasets. We refer to the connected transformed dataset as the pre merged dataset (ESI 6).

Statistical analyses. All statistical analyses were performed with the R software version 3.6.2 and the "ggplot2", "ade4", "MASS", "corrplot", "MVN" packages (Chessel et al., 2004 ; Wickham, 2011; Ripley et al., 2013 ; Korkmaz et al., 2014 ; Wei et al., 2017) . Used scripts are provided in supplementary data (ESI 7).

We tested the multivariate normality of our raw data with the Mardia's multivariate skewness and kurtosis test, Royston's multivariate Shapiro–Wilk test and the Henzee Zirkler empirical characteristic function test using the MVN statistical package for the R programming environment (Korkmaz et al., 2014 ; Cain et al., 2017) . All three MVN tests found that our data sets are non-multivariate normal. As LDA has been considered as robust to violations of data set multivariate normality, we pursued our analysis (Blanca et al., 2013 ; Enserro et al., 2019). The use of logarithm scaling decreases the existing bias due to the difference of scale of concentration between the distinct elements under consideration (Baxter, 1994 ; MacDonald et al., 2018). For ochre sourcing studies as ours, such a transformation is essential, given the difference of magnitude between the major, minor and trace elements. Moreover, the log transformation allows the reduction of the multivariate non-normality of the measures distribution and increases the robustness of the statistical performance (Buxeda i Garrigós, 2018) .

After these treatments we used Principal Components Analysis (PCA) and Linear Discriminant Analysis (LDA). To evaluate the performance of LDA on the different datasets considered, we performed cross-validations tests. The cross-validation tests were based on calculation of the confusion matrix using the confusion function published by Maindonald and Braun (2006) . It is calculated from predictions of class membership that are derived from leave-one-out cross-validation and comparison of the actual given and predicted group assignments.

3.RESULTS

3.a. Standards and techniques performances

Major elements. Raw concentrations measured on the DRN, BXN and IFG standards are presented in Table 2.

Table 2. Certified and mean measured concentrations of major and minor elements for the DRN, BXN and IFG standards (% wtO). (NM: non measured, LOD: Limit of Detection, * standard deviation not provided by reference material certificate, ** standard deviation < 0,1 %).

Standard	Analytical technique	Na_2O	MgO	Al_2O_3	SiO_2	CaO	K_2O	TiO_2	Fe_2O_3
BXN	Certified	0.1	0.1	54.2 ± 1.2	7.4 ± 0.5	0.2 ± 0.1	<0.1*	2.4± 0.2	23.2 ± 0.8
	ICP (OES)	<0.1*	0.1 *	61.7 ± 0.2	8.2 ± 0.1	0.3 ± 0.1	<0.1	2.6*	26.8 ± 0.1
	PIXE	<LOD	0.3 ± 0.1	60.8 ± 1.1	9.6 ± 0.3	0.3 ± 0.2	<0.1*	2.7 ± 0.1	25.5 ± 0.6
	pXRF	NM	NM	47.9 ± 1.6	7.1 ± 0.1	0.2 *	<0.1*	2.4 ± 0.1	24.3 ± 1.0
DRN	Certified	3	4.4	17.5 ± 0.6	52.9 ± 0.7	7.1 ± 0.2	1.7 ± 0.1	1.1 ± 0.1	9.7 ± 0.3
	ICP (OES)	3*	4.4*	17.8 ± 0.1	54.1 ± 0.3	7.1*	1.7 ± 0.2	1.1 *	9.7*
	PIXE	3 ± 0.1	4.2 ± 0.2	17.7 ± 0.3	52.9 ± 0.8	6.9 ± 0.2	1.7**	1.1 ± 0.1	10.0 ± 0.5
	pXRF	NM	NM	21.2 ± 9.8	56.9 ± 15.0	7.0 ± 1.1	1.9 ± 0.3	1.0 ± 0.1	11.8 ± 1.4
IFG	Certified	<0.1**	1.8 ± 0.2	0.2 ± 0.1	41.2 ± 0.7	1.6 ±0.2	<0.1*	<0.1*	55.9 ± 0.1
	ICP (OES)	<0.1**	1,8**	0.2*	40.4 ± 0.2	1.4*	<0.1*	<0.1*	55.7 ± 0.1
	PIXE	0.4 ± 0.2	2.2 ± 0.2	0.3*	39.0 ± 0.7	1.5 ± 0.1	<0.1*	<0.1*	55.0 ± 0.7
	pXRF	NM	NM	3.2 ± 0.5	43.7 ± 8.6	1.9 ± 0.1	<0.1*	<0.1*	53.8 ± 3.2

For ICP-OES, most standard deviations are low, often below 0,01 % (Table 2), thanks to the good repeatability of the technique. Most ICP-OES measures fall within the incertitude range of the certified values. Discrepancies are observed for major elements (Al_2O_3, SiO_2, Fe_2O_3) for standard BXN, a standard with a loss of ignition of 11.5 %. LOI for DRN and IFG are 2.2 and -1.1% respectively. Thus, the discrepancies could be related to the high LOI of the BXN.

PIXE concentrations present similar accuracy and discrepancies that seems related to the LOI (Table 2). Configuration parameters used for concentration computation using GUPIX software were tested on samples with low LOI, including DRN. Measurements of a sample with a higher LOI as BXN do not appear accurate (Table 2).

pXRF results are close to the certified values and fall within their incertitude range. They present higher discrepancies with the certified concentrations than PIXE and ICP-OES ones (Table 2). Major discrepancies exist for all three standards for Al_2O_3 content. This is imputable to the low weight of the element and the existence of some overlapping with L and M bands of heavier elements. Though the measures acquired the three techniques are of the same estimate, possibly allowing their comparison.

Trace elements.

Most trace elements (As, Ba, Cu, Cr, Ga, Mn, Ni, Pb, Rb, Sr, V, W, Y, Zn) confirm the previous results: good accuracy and repeatability of PIXE and ICP-OES and lower accuracy and repeatability for pXRF (Table 3). Most measures fall within the range of uncertainty of the certified values. LOD of PIXE and pXRF non-destructive are higher than the ones of ICP-MS and ICP-OES for most elements (Table 3). The high LOD of PIXE for Cr is due to the use of a Cr filter. Sulphur concentrations appeared highly inaccurate and unprecise for all the techniques used in our study. Therefore, we did not consider this element in our following analyses.

Contrary to Chanteraud et al. (2021), who did not calibrate their pXRF, unifying the data sets seems possible. Therefore, we decided to investigate the possibility to unify these different measures despite the existing discrepancies.

Table 3. Certified and mean measured concentrations of trace elements for the DRN and BXN standards in ppm. (NM: non measured, LOD: Limit of Detection, *standard deviation not provided by standard certificate, ** standard deviation < 1 ppm, *** existing discrepancies between literature and standard certificate).

Standard	Analytical technique	As	Ba	Cu	Cr	Ga	Mn	Ni	Pb	Rb	Sr	V	W	Y	Zn	Zr	S
BXN	Certified	115 ± 9	30 ± 7	18 *	280 ± 75	67 ± 19	387 ± 155	180 ± 37	135 ± 77	3 ± 11	110 ± 19	350 ± 77	9 *	114 ± 40	80 ± 39	590 ± 86	NM
	ICP-MS	115 ± 7	24 ± 3	19 ± 1	270 ± 1	67 ± 5	NM	175 ±10	153 ± 28	4 ± 1	110 ± 4	343 ± 2	NM	94 ± 2	77 ± 4	298 ± 3	NM
	ICP-OES	NM	41 ± 5	10 ± 2	268 ± 5	NM	509 ± 5	NM	NM	NM	109 **	355 ± 3	<LOD	NM	86 ± 5	329 ± 13	372 ± 249
	PIXE	130 ± 8	<LOD	14 ± 3	<LOD	70 ± 5	384 ± 31	204 ± 18	163 ± 13	2 ± 4	124 ± 6	462 ± 79	<LOD	112 ± 5	87 ± 8	567 ± 96	1414 ± 1787
	pXRF	174 ± 71	<LOD	<LOD	328 ± 18	46 ± 2	522 ± 122	218± 14	146 ± 14	6 ± 5	72 ± 7	348 ± 21	<LOD	61 ± 3	55 ± 3	580 ± 30	NM
DRN	Certified	3 ± 1	385	50 ± 7	40 ± 11	22 ± 5	1704 ± 155	15 ± 11	55± 7	73 ± 8	400 ± 50	220*	130 *	26 ± 7	145 ± 17	125 ± 25	350
	ICP-MS	3 **	368 ± 33	45 ± 3	34 ± 1	22 ± 1	NM	16 ± 1	53 ± 9	70 ± 3	386 ± 5	205 ± 2	NM	26 ± 1	134 ± 2	26 ± 1	NM
	ICP-OES	NM	375 ± 6	45 ± 1	36 ± 2	NM	1685 ± 52	NM	NM	NM	393 ± 3	208 ± 2	114 ± 7	NM	140 ± 4	24 ± 1	1048 ± 623
	PIXE	4 ± 3	300 ± 188	54 ± 7	<LOD	22 ± 3	1787 ± 103	<LOD	61 ± 9	72 ± 4	399 ± 19	219 ± 44	136 ± 8	23 ± 4	155 ± 9	99 ± 50	7044 ± 1420
	pXRF	<LOD	337 ± 180	46 ± 6	<LOD	24 ± 2	2235 ± 259	<LOD	37 ± 7	73 ± 6	427 ± 40	180 ± 34	129 ± 8	18 ± 1	156 ± 6	186 ± 16	NM
IFG	Certified	2 ± 1	2*	10 ± 3	9 ± 3	1*	325 ± 108	23 ± 16	4*	1*	3*	2*	220 ± 60***	9*	20 ± 7	1*	700*
	ICP-MS	1**	<1**	13 ± 1	9**	<1**	NM	26 ± 1	4 ± 1	1**	<1**	4**	NM	8**	20 ± 5	4**	NM
	ICP-OES	NM	11 ± 7	3 ± 2	11 ± 3	NM	318 ± 30	NM	NM	NM	3 ± 4	7 ± 5	44 ± 18	NM	45 ± 2	8 ± 1	1612 ± 925
	PIXE	6 ± 1	<LOD	10 ± 3	<LOD	<LOD	323 ± 40	<LOD	1 ± 2	<LOD	<LOD	<LOD	<LOD	8 ± 5	26 ± 2	2 ± 2	230 ± 326
	pXRF	<LOD	<LOD	<LOD	<LOD	<LOD	471 ± 217	27 ± 14	<LOD	<LOD	<LOD	<LOD	75 ± 42	<LOD	26 ± 12	<LOD	NM

3.b. ICP-OES and ICP-MS results

We already demonstrated the possibility to differentiate ferruginous colouring matter from five different tectonostratigraphic zones thanks to ICP-OES/ICP-MS and multivariate statistics (Mauran et al., 2021a). Among the five zones discriminated in our previous study, are the three zones studied in the present study.

For the present study, 55 samples were analysed both by ICP-OES and ICP-MS (Table 1). Raw elemental concentration data are provided in ESI 4. We first aimed to confirm the possibility to differentiate the three zones thanks to ICP-OES and ICP-MS data. Therefore, ICP-OES/ICP-MS centred-log-ratio transformed data were submitted to principal component analysis and linear discriminant analysis for the following elements: Al, Ca, Fe, K, Mn, P, Si, Ti, Cr, Ni, Zn, W, Cu, Y, As, Sr, Zr, Mo, Ga, Pb.

Biplots of the first two principal components are plotted in Fig. 3 and component loadings are given in ESI 8. For PCA (Fig 3.A), the first two components account for 44,8 % of the total variation, and are mostly driven by Cu, Ni, Cr, As, Zr, Pb, Ti, Sr, Mn, Fe, P. The different samples from the three distinct zones are grouped according to their provenance. They form three distinct clusters with no overlap between their 80% significance level ellipses (fill) and minor overlaps between their 95% significance ellipses (dash). It confirms the possibility to distinguish the provenance of the samples from their geochemical signature.

Discrimination performed by LDA (Fig 3.B), for which the first axis accounts for 54.2 % and the second for 45.8 %, is mostly driven by As, Cr (axis 1), K and Mn (axis 2) (ESI 8). Samples from the three distinct zones are grouped according to their provenance forming three distinct groups with no overlap between their 95% significance ellipses, making it a good model for sourcing ferruginous colouring matters. LDA cross-validation provided a score of 87.3 % of correct attribution, confirming the effectiveness of the model to discriminate the distinct zones.

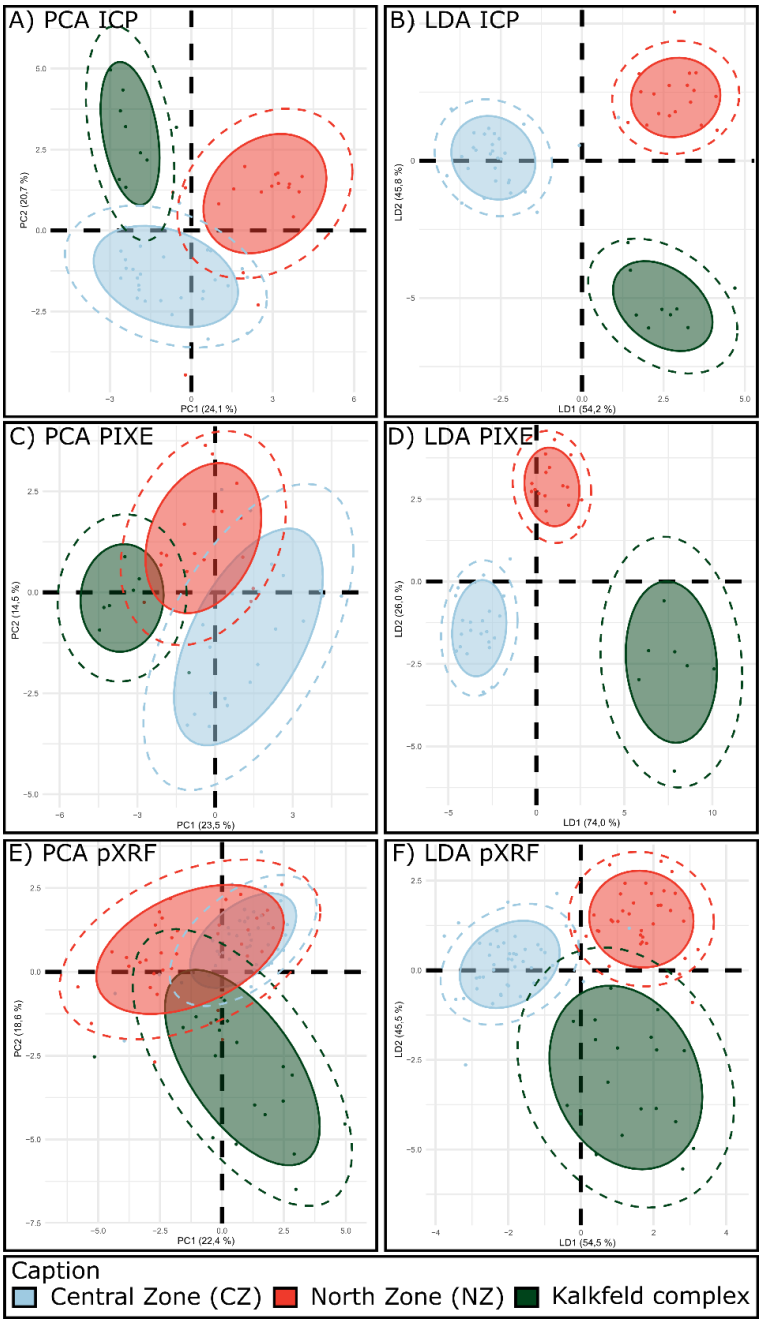

Fig. 3. Principal component analyses (left) and linear discriminant analysis (right). A-B: ICP data; C-D: PIXE data; E-F: pXRF data;. 80% significance level ellipses (fill) and minor overlaps between their 95% significance ellipses (dash). (double column, colour)

3.c. PIXE results

In total, 23 samples were analysed by PIXE (Table 1). Raw elemental concentration data are provided in ESI 2. PIXE centred-log-ratio transformed data were submitted to principal component analysis and linear discriminant analysis for the same elements that those used for ICP data treatment.

Biplots of the first two components are presented in Fig 3.C and component loadings are given in ESI 7. For PCA (Fig. 3.C), the first two components account for 38 % of the total variation, mostly driven by Cr, As, Zr, Sr, Al, Mn, Zn, Ga. Though samples from the three distinct zones are grouped according to their provenance forming three identifiable poles, there are minor overlaps between the 80 % significance level ellipses and rather large overlaps between the 95% ellipses.

Discrimination performed by LDA (Fig. 3.D), for which the first axes accounts for 74 % and the second for 26 %, is mostly driven by Zn for both axes (ESI 9). Samples from the three distinct zones are grouped according to their provenance forming three distinct groups with no overlap between their 95% significance ellipses, making it a good model for sourcing ferruginous colouring matters. LDA cross-validation for the PIXE datasets provided a score of 84.8% of correct attribution. Though smaller than the ones obtained for ICP, the two cross-validation scores remain of same magnitude.

3.d. pXRF results

In total, 52 samples were analysed by pXRF (Table 1). Raw elemental concentration data are provided in ESI 1. We first aimed to confirm the possibility to differentiate the three zones thanks to pXRF data. Therefore, pXRF centred-log-ratio transformed data were submitted to principal component analysis (PCA) and linear discriminant analysis (LDA) with the same elements as for the two precedent analytical techniques.

Biplots of the first two components are presented in Fig 3. E and component loadings are given in ESI 10. The two first PCA components account for 41 % of the total variation of the data, mostly driven by Fe, Cu, Pb, K, Sr. Though the Kalkfeld samples stand out from CZ and NZ on the PCA biplots, there are major overlaps between the 80 % significance level ellipses. The PCA performed on the "pXRF centred-log-ratio" data (pXRF clr) fails to differentiate the three zones studied here.

Discrimination performed by linear discriminant analysis (LDA) (Fig. 3. F), for which the first axes accounts for 54.5% and the second for 45.5%, is mostly driven by Al, Zn, Cu for both axes (ESI 10). Samples from the three distinct zones are grouped according to their provenance forming three distinct groups with no overlap between their 80% significance level ellipses (fill) and minor overlaps between their 95% significance ellipses (dash). LDA cross-validation for the pXRF datasets provided a score of 70% of correct attribution. Smaller than the two previous cross-validation scores, the cross-validation score also confirmed the lesser efficiency of the LDA with the pXRF data to discriminate the distinct zones.

3.d. Comparison of the datasets: Inter-equipment *versus* inter-zone variability

We thence investigated the possibility to compare these datasets, evaluate the inter-equipment and inter-zone variability. We first used our centred-log-ratio transformed dataset (clr) and submitted it to

principal components and linear discriminant analyses. Linear discriminant analyses factor consisted in the analytical technique used to measure the samples and the area of provenance of the samples (Fig. 4). PCA and LDA biplots are presented in Fig. 4 and variable loadings in ESI 11 and 12.

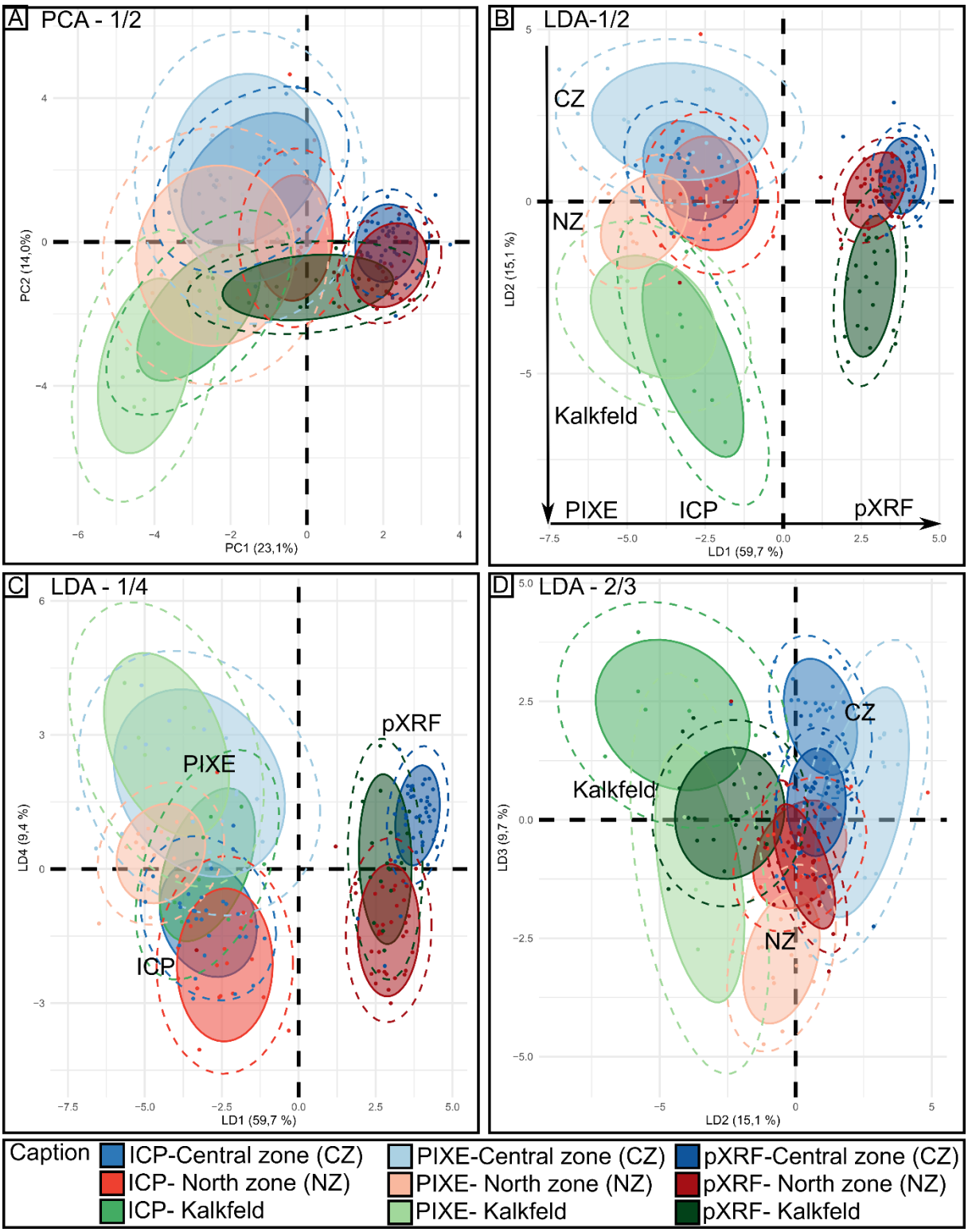

Fig. 4. Principal component analysis (A) and linear discriminant analysis (B-D) of the post merged standardized datasets from ICP, PIXE and pXRF. 80% significance level ellipses (fill) and minor overlaps between their 95% significance ellipses (dash). (double column, colour)

Biplot of the first two components of the PCA accounts for 37.1 % of the total variation of the data (Fig.4.A). While the first component (23.1 %) mainly explains inter-equipment variability thanks to Ca, Cr, Fe, Mn and W, the second component (14.0 %) tends to explain some inter-zone variability thanks to Ti, Sr, Cu, Ni (ESI 11). From this biplot, it is clear that within the post merged standardized dataset, the inter-equipment variability is higher than the inter-zone variability.

Biplots of the first four axes of the LDA help to go further into the analysis of the inter-equipment and inter-zone variabilities (Fig 4.B-D). Two different trends appear on the LD1-LD2 biplot, one driven by LD1 takes the inter-equipment variability, while the other one driven by LD2 takes the inter-zone variability (Fig 4.B). On the LD1-LD4 biplot, two major poles tend to form according to the analysis used to acquire the data pXRF on one side and PIXE and ICP on another (Fig. 4.C), while on the LD2-LD3, the three poles correspond to the three zones of provenances of the samples (Fig. 4.D). While LD1 (59.7 %) and LD 4 (9.4 %) explains the inter-equipment variability, LD2 (15.1 %) and LD3 (9.7 %) explains the inter-zone variability. The cross-validation performed thanks to the two first axes of the LDA reached a score of 64.5%. In this case, 69.1 % of the dataset variation accounts for the inter-equipment variability. In such conditions, centred-log-transformed normalisation is not suitable to compare the data acquired by the different techniques.

As we wanted to understand which elements were driving the two different sources of variability of the datasets, we analysed both the variance of the elements according to the analytical techniques used to measure them and the mean values of each group defined as the combination of the zone of provenances of the samples and the techniques used to analyse it. Results of these considerations are presented in Fig. 5.

It appeared that the different analytical techniques presented different variances for each element. Indeed, while iron and potassium displayed similar variance values around 0.5 for the three techniques, the variances for P, Si, Ti, Ni, W and Cu present significant differences, ranging between 0.1 and 3.0 (Fig. 5.A).

Bar plot of the mean values of each of the nine groups defined (three zones and three analytical techniques) permitted to confirm the two trends spotted on the LDA loadings, confirming Al, Ca, Fe, K, Cr and W to be highly impacted by inter-equipment variability, while Si, Ni, Zn, Cu and Sr appeared to discriminate more the zone of provenances of the samples (Fig. 5.B, ESI 12).

Though the inter-equipment variability of the post merged standardized dataset is too important to be used to compare the samples analysed by the different analytical techniques, a part of the variance appears to be driven by the geochemical properties of the provenance zones of the colouring matters.

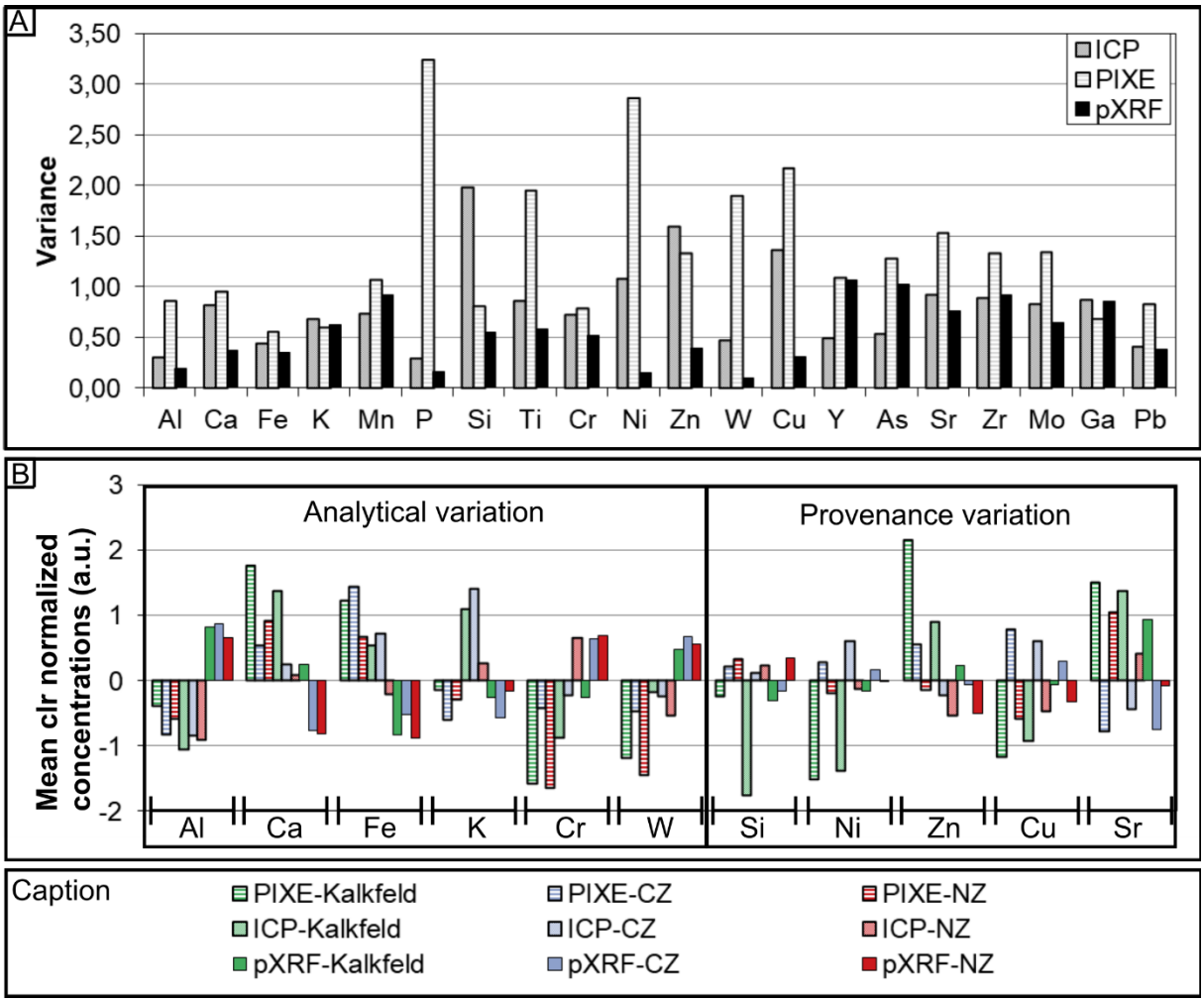

Fig. 5. A: Elemental concentration variance for each technique (ICP, PIXE and pXRF); B: Elemental variance for each technique and provenance zone on the post merged standardized dataset. (double column, colour)

3.e. Unification of the datasets

As demonstrated in the previous section, inter-equipment variability can be unneglectable and can induce a wide range of variance values for the same element. We standardize here each dataset separately before merging them. This procedure is a standardization that rescales the data sets to ensure the mean is 0 and the standard deviation 1. Corresponding PCA and LDA biplots are presented in Figure 6 and variable loadings in ESI 11 and 12.

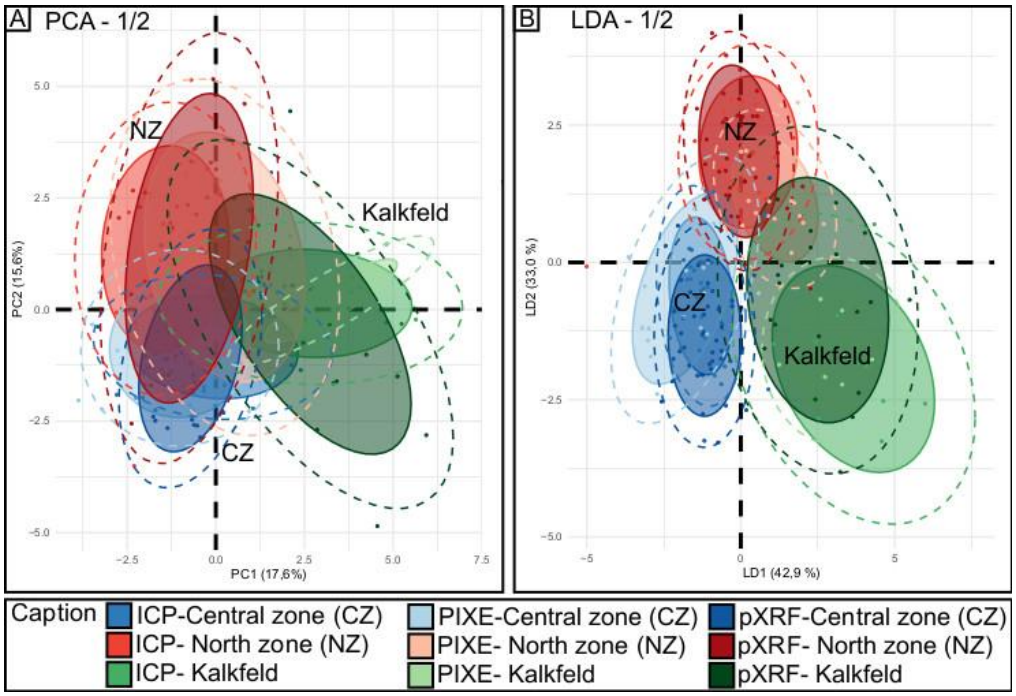

Fig. 6. Principal component analysis (A) and linear discriminant analysis (B) of the pre merged standardized datasets established by ICP, PIXE and pXRF. 80% significance level ellipses (fill) and minor overlaps between their 95% significance ellipses (dash). (double column, colour)

Biplot of the first two components of the PCA accounts for 33.2 % of the total variation of the data. Though there are major overlaps between the 80% significance level ellipses, three poles appear on the PC1-PC2 biplot. These three poles correspond to the zones of provenance of the samples. While the first component (17.6 %) mainly differentiates the Kalkfeld zone from the two others thanks to Cr, Ca, Mn, Sr, As, Zn, the second component (15.6 %) tends to differentiate the NZ and CZ zones thanks to Fe, Ti, Zr, Si, Cu (ESI 11). These biplots demonstrate that inter-equipment variability can be minimized by applying a standardization procedure of each dataset acquired with each technique before merging them.

As for the LDA, the LD1-LD2 axes account for 75.9 % of the total variation of the data. Although we tried to distinguish nine groups, and despite a slight overlap of the 80% significant level ellipses for Kalkfeld pXRF and NZ data, three poles can be distinguished according to the zone of provenances of the samples (Fig. 6). The cross-validation performed on the two first axes of the LDA reached a score of 75.2%, even reaching 82.5% when all axes are considered. Thus, the standardization considerably increased the discrimination of the zones, reaching the same cross-validation score magnitude than what had been obtained for ICP or PIXE alone. It allows a comparison of the data acquired with the different analytical techniques.

Bar plot of the variance values of each of the nine groups defined (three zones and three analytical techniques) permitted to confirm that the standardization procedure permitted to minimize the inter-

equipment variability (Fig. 7). After the standardization procedure, none of the elements highlighted an inter-equipment variability, while eight elements differentiated the groups according to the provenance zones of the samples. Elements such as Ca and Fe, which were highly impacted by the inter-equipment variability, even contributed to differentiate the zone of provenances of the samples.

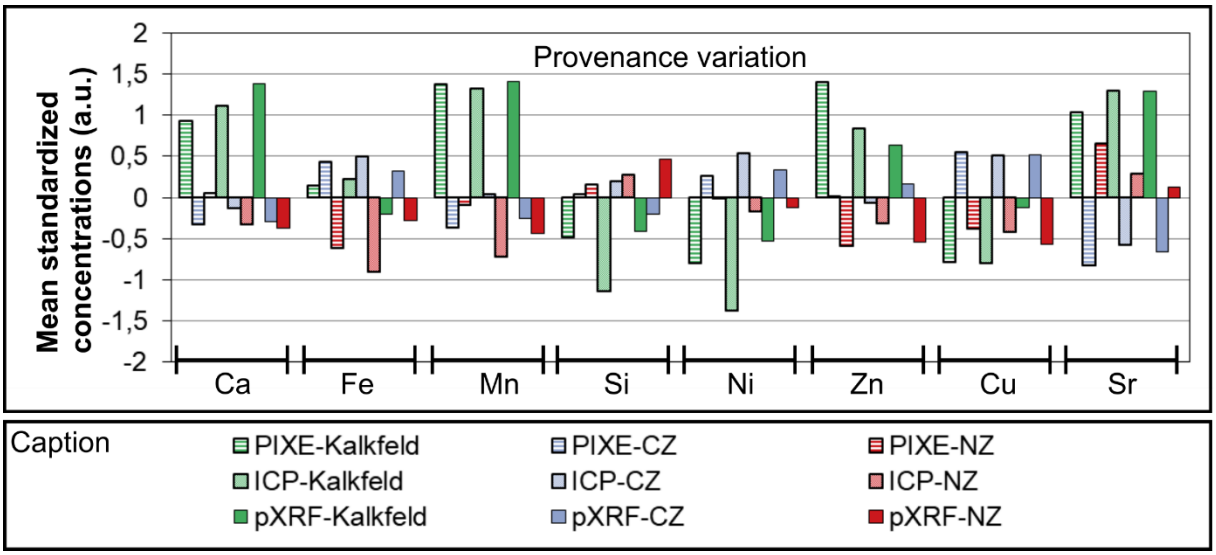

Fig. 7. Elemental variance for each technique and provenance zone on the pre merged standardized dataset. (double column, colour)

4.DISCUSSION

Measures performed on standards (diorite DRN, bauxite BXN and iron formation IFG) confirmed ICP-MS is the most accurate and repeatable analytical technique (Table 3), followed by ICP-OES and PIXE. pXRF measured data present some discrepancies with the certified values, as already stated in the literature (Hein et al., 2002). Although the discrepancies observed for the two standards are weak, it appeared that data acquired with these techniques were not directly comparable. This is not surprising as inter-laboratories and sometimes day to day measure on a same equipment are not directly combinable (Yellin et al., 1978 ; Popelka-Filcoff et al., 2012 ; Salomon et al., 2016)..

Published comparisons of data acquired by sundry techniques usually compare the performances of each analytical techniques to differentiate for example ceramic workshops (Hein et al., 2002 ; Grave et al., 2005 ; Speakman et al., 2011 ; Mitchell et al., 2012) or mineral outcrops (Kasztovszky et al., 2018). They all tend to prove the consistency between the cluster performed thanks to NAA, ICP-OES/ICP-MS, PIXE and pXRF analytical methods. Here we demonstrate this consistency to be also true for Namibian ferruginous colouring matters. We go further by comparing the datasets, allowing us to determine the importance of the elemental inter-equipment and inter-zones variabilities.

Application of the centred-log-ratio transformed data and multivariate statistics revealed that ICP-OES/ICP-MS and PIXE analyses could differentiate the Namibian samples according to their zone of

origin (Fig. 2). Using pXRF measurements, three distinct poles corresponding to the three zones of origin of the samples considered in our study can be observed, slightly overlapping each other. Though quick to acquire, pXRF analyses require time and efforts to quantify the elemental composition of ferruginous colouring matters (Speakman et al., 2013). Having the possibility to compare them with other techniques compensates in some views the time and efforts invested to process them.

In a recent paper, Chanteraud and colleagues (2021) investigated the capacities of pXRF to study the "*chaîne opératoire*" of ferruginous colouring matters. They compared pXRF data to PIXE and ICP data as well and conclude that it is currently not possible to directly use pXRF data to accurately quantify the elemental content of colouring matters or to discriminate different raw materials. Our study confirms the difficulty to compare the concentration calculated with pXRF with the results obtained with PIXE or ICP-MS. The comparison of raw closed and merged data show that the analytical inter-equipment variability accounts for most of the total variability of the data (Fig. 3). Compositional differences related to geological discriminations can exist. They are partially masked by the preponderant inter-equipment variability. This inter-equipment variability is mainly due to the difference of measurement principles between the distinct techniques used, leading to analyse different volumes, to make some elements difficult to measure.

This does not mean that some of our data are invalid as explained by Bernard (2017). Scales between the measures might be different and therefore need to be corrected, so they can be considered valid and compatible with other data. As we noticed differences between the determined variances of the elements according to the analytical techniques (Fig. 5), we standardized our data according to the analytical technique used so that all elements present a variance equal to one. This standardization was performed separately for each dataset collected through distinct analytical techniques. Doing so minimized the inter-equipment variability and allowed a comparison between the data acquired by pXRF, PIXE and ICP-OES/ICP-MS (Fig. 6). Two facts must be noticed: 1) we did not reduce our number of variables, consequently favouring better discrimination of the groups, not only according to the provenance of the samples but also the techniques used to perform the measures; 2) we used centred log-ratio transformed data so that the study is robust to the fact we analysed sub-compositions of our samples (Aitchison, 1982 ; Baxter et al., 2005). As our study is robust to sub-composition statistical analyses, a similar conclusion could be obtained with the Fe log-ratio transformation usually used in ferruginous colouring matter sourcing studies (David et al., 1993 ; Popelka-Filcoff et al., 2007, 2008).

Such a geochemical discrimination study is largely favoured by the geological context of Central Namibia, characterized by different tectonostratigraphic regions. Here, we analysed materials coming from three of the central Namibian tectonostratigraphic regions: Central Zone where lies numerous rock art sites such as Leopard Cave, Kalkfeld complex located 100 km north to Leopard Cave, and North Zone located at more than 100 km north-west from Leopard Cave (Figure 1). Our previous study has

proved, some of the collected but unmodified colouring matters recovered at Leopard Cave come from the Central Zone and the North Zones (Mauran et al., 2021a) . Thanks to the present standardization procedure, integration of other tectonostratigraphic zones could be implemented in the future. Using the standardization procedure on Leopard Cave materials, rich of numerous massive haematite (Mauran et al., 2020) , would allow us to understand better if past populations who occupied the site preferred to use specific massive haematite and if different haematite were used for different purposes, thus providing a better understanding of past populations behaviours. It would be interesting to investigate the possibility to perform such a comparison at a lower geographical level within the different tectonostratigraphic zones to differentiate the sundry outcrops. The present unification is already of great help since it allows us to investigate the possible existence of large procurement networks of raw colouring matters in Namibia. Investigating if such unification could be performed in a different geological context would be of higher interest, it could help us to ensure the standardization procedure is robust.

It is worth mentioning that our standardization procedure should be only deployed in other contexts and on other materials after ensuring that standards and references analysed through the different analytical techniques considered are comparable. The standardization procedure is then a way to include modified and unmodified ferruginous colouring matters in provenance studies, which allows a better understanding of past populations behaviours towards the exploitation of these raw materials.

This comparison of the datasets acquired by distinct analytical techniques opens the possibility to establish a geochemical provenance model of Namibian ferruginous colouring matters from different analytical techniques. Large assemblages of archaeological materials are usually screened by the non-invasive and easily accessible pXRF technique. Our standardization procedure allows the integration of these pXRF data to provenance study and validates the coherence of performing such pre-screening analyses for ferruginous colouring matters as sometimes performed for iron slags (Vega et al., 2019) . pXRF data were acquired with an equipment calibrated thanks to 21 standards, most of which did not match the composition of the geological samples. With the use of standards matching better the composition of the considered samples, the pXRF accuracy should be improved,

Using the pXRF technique on both geological and archaeological collections would provide some first data to better understand the samples. In specific context such the one studied by Lebon and colleagues (2019), pXRF can reveal specific geochemical patterns. These patterns could be further investigated and confirmed on a smaller batch of samples, wisely selected from petrographic observations and pXRF analyses, through invasive techniques such as ICP-OES/ICP-MS or NAA. Thence, it is possible to compare these precise geochemical signatures with data acquired on archaeological samples, chosen thanks to reasoned sampling strategy using pXRF pre-screening results, with both non-invasive analytical techniques such as PIXE for the samples presenting anthropic modifications and invasive

techniques for some unmodified archaeological pieces. Thus, the pXRF could help researchers to perform their sampling procedure for the time or fund costly analyses such as ICP-OES/ICP-MS or NAA. Naturally, these techniques should then be combined with other analytical methods such as petrography or X-ray diffractometry. Such multimodal approaches are the way to go to understand as much as possible the "*chaîne opératoire*" of ferruginous colouring materials exploitation (Dayet, 2021 ; Domingo and Chieri, 2021).

Furthermore, our standardization procedure could offer a way to compare data derived from different non-invasive and invasive analytical techniques on the same colouring matter fragments. Doing so, it would permit to take the best of each technique. Indeed, it would then be possible to take advantage of the accessibility, rapidity, portability and non-invasiveness of the pXRF, or of the accuracy, spatial resolution and non-invasiveness of the PIXE together with the accessibility, micro-destructive, high-precision and rapidity of the ICP-OES and ICP-MS. Thanks to this data unification, it would thence possible to have a better understanding of large ferruginous colouring matter assemblages, the first step toward a better understanding of the "*chaîne opératoire*" link to these materials. It would thence here possible to have an accurate knowledge of the chemical fingerprint of the potential sources and compare it to some non-destructive PIXE analyses carried out on archaeological pieces.

Future studies should focus on ferruginous residue analyses thanks to PIXE and LA-ICP-MS/MS (or NAA) and the way to compare them with ferruginous colouring samples to offer a way to study the whole "*chaîne opératoire*" linked to ferruginous colouring matter as presented in Fig. 1. These developments should be carried out together with petrological and SEM observations to offer robust ways to study ferruginous colouring matters (Dayet et al., 2013 ; Salomon et al., 2016) . Used together with these developments, our standardization procedure offers a way to set up a robust "grain per grain" microscopic methodology. This methodology could tackle the intrinsic heterogeneity of ferruginous colouring matter, through the multiplication of the analyses on the same sample as mentioned for LA-ICP-MS by Scadding and colleagues (2015).

Finally, such a standardization allows comparison of compositional datasets acquired by distinct users, increasing the interoperability of the datasets, a key idea of the FAIR concept (Findable, Accessible, Interoperable, Reusable) for better practices in science. With our standardization procedure, it is possible to minimize the inter-equipment variability, including the inter-operators one, and compare datasets from different origins. Therefore, our standardization offers a new way to increase the interoperability and reusability of the datasets acquired at different laboratories or by different teams, which has been a preoccupation for archaeometry laboratory in the last two decades (Glascock et al., 2004). Naturally, to do so it is of utmost importance to use the same standards between the datasets to be compared, as already mentioned by Salomon and colleagues (2016). Comparison of the standards will confirm that on similar samples the data acquired on distinct equipment are coherent and comparable.

5.CONCLUSIONS

In this article, we first investigated the issue of data standardization to compare elemental analyses acquired by distinct analytical techniques. Second, we tested the efficiency of each technique to discriminate the source of ferruginous colouring matter sampled in three different geological zones when coupled to multivariate statistical analyses. Third, we evidenced how the datasets can be incompatible though they are precise and accurate. Fourth, we demonstrated the possibility to merge the multivariate analyses through a basic data transformation. Five, we discussed the archaeological implication and limitation of our methodology.

The results of the study indicated that using the presented standardization of the measured elemental concentrations could be used to obtain a unified dataset in which inter-equipment variability is negligible. In doing so, it allowed the use of multivariate analyses to differentiate Namibian ferruginous colouring matter provenance.

Moreover, it opens the way for building a multi-analytical provenance model. Such a multi-analytical provenance model would gather more analyses than the ones usually performed and relying on a unique invasive technique (Kiehn et al., 2007 ; Popelka-Filcoff et al., 2007, 2008 ; Dayet et al., 2013 ; Eiselt et al., 2011 ; MacDonald et al., 2013, 2018 ; Pierce et al., 2020 ; Dayet, 2021). Overcoming this number limitation is crucial to perform more robust provenance studies for ferruginous colouring matter on the model of what has been done for iron slags in metallurgy (Leroy, 2010 ; Leroy et al., 2012). Such studies do not only rely on a sole generic multivariate analysis but go beyond evaluating for each sample the statistical possibility that a sample can come from a specific mining region. Doing so, better take into account the possibility that some outcrops used by past populations are nowadays depleted. As the statistical tests used to do so (mainly linear discriminant analysis) require the comparison of distinct distributions (ideally normal distributions), each archaeological sample should be represented by a distribution of analyses. The cost and time required to do this with a unique invasive technique are tremendous and explain why it has so far never been performed. Through this unification procedure, each archaeological sample could easily be represented by a distribution. As we are convinced, studies on ferruginous colouring matters should go towards this direction, our future research will focus on the possibility to use our multi-technical tectonostratigraphic zone discrimination model to perform such provenance analyses. However, comparing and unifying the data is different than performing provenance analyses and further work are necessary to ensure such an approach would fulfil the Provenance Postulate (Weigand, 1977).

Beyond the possibility to perform robust provenance studies, this unification of the datasets allows provenance studies to be anchored into the investigation of ferruginous colouring matters evolutive chain as defined for siliceous resources by Fernandes and colleagues (2008) . Such an approach is crucial

when studying the social-cultural behaviours of past populations. As stated by Fernandes and colleagues (2008), identifying characteristic specific to secondary beds, called “gitological types” is more useful than “genetic types” which depend upon the initial geological formations from which the ferruginous colouring matter come from for provenance studies. To this aspect, our results are crucial for general geochemical analyses studies of archaeological materials and cultural material analyses. Our result will enable inter-study comparisons of new analytical techniques or procedures applied to sourcing research and existing techniques applied to new materials or geographic regions.

CONFLICT OF INTEREST STATEMENT

There are no conflicts to declare.

AUTHOR CONTRIBUTIONS

Conceptualization: GM, ML, LB, FD, BC, DP, JJB, CN

Data curation: GM, BC, ML

Formal analysis: GM, BC, LB, ML

Funding acquisition: ML, DP, JJB, BC, LB

Investigation: GM

Methodology: GM, ML, LB, FD, BC, JJB, CN

Project administration: GM, ML, BC, DP, JJB

Resources: GM, OT, ML, BC, FD, DP, LB, CN

Supervision: ML, JJB

Validation: BC, ML, FD, JJB, LB, OT

Visualization: GM

Writing – original draft: GM

Writing – review & editing: GM, ML, JJB, FD, DP, BC, LB, OT

ACKNOWLEDGEMENTS

The authors are very grateful to Ms and Mr Rust and their family for their kind permission to access and excavate the archaeological site of Leopard Cave, located on their farm.

This research was supported by grants from the French Ministry of Foreign Affairs through the project "MANAM: Mission Archéologique en NAMibie", the LaBex BCDiv (Biological and Cultural Diversity) for the project "Dynamique des peuplement en Namibie à l'Holocène - NAMIBIE (Windhoek, Erongo)" both directed by D.P., the Observatoire des Patrimoines de Sorbonnes universités (OPUS) through the project "APaNam: Art rupestre et Patrimoine en Namibie" directed by M.L. Research by G.M. was funded by the Chaire Polyre of Sorbonnes Universités.. Permission to conduct research was granted by the National Heritage Council of Namibia (permit 11/2015 and permit renewal 04/2017 given to D.P.) and the Namibian Ministry of Mine and Energy (permit ES 31957 granted to G.M.). We are grateful for the support and assistance of this institution as well as the National Museum of Namibia, the National Heritage Council, the Geological Survey of Namibia and the French embassy in Namibia. We are grateful to Quentin Pichon and Clare Pachecaud for the help with the air-extracted PIXE analyses at the NEWAGLAE facility. We also acknowledge the two anonymous reviewers who helped us improve the manuscript.

GM acknowledges the support of the DSI-NRF Center of Excellence in Paleosciences (CoE-Pal) towards his postdoctoral work when this paper was written and corrected. Opinions expressed and conclusions arrived at, are those of the author and are not necessarily to be attributed to the CoE. Opinions expressed and conclusions arrived at, are those of the authors and are not necessarily to be attributed to the CoE.

ONLINE DATA

[dataset] Mauran, G., Caron, B., Détroit, F., Nankela, A., Bahain, J.-J., Pleurdeau, D., Lebon, M., 2021b. Namibian reference ochres description and geochemical data [Data set]. Zenodo. http://doi.org/10.5281/zenodo.3908304.

REFERENCES

Aitchison, J., 1982. The statistical analysis of compositional data. Journal of the Royal Statistical Society: Series B (Methodological), 44(2):139–160. https://doi.org/10.1111/j.2517-6161.1982.tb01195.x.

Aitchison, J., 1986. The Statistical Analysis of Compositional Data. Monographs on Statistics and Applied Probability. London, Chapman, & Hall Ltd.

Baxter, M. J., 1994. Exploratory multivariate analysis in archaeology. Edinburgh University Press.

Baxter, M. J., 1995. Standardization and transformation in principal component analysis, with applications to archaeometry. Journal of the Royal Statistical Society: Series C (Applied Statistics), 44(4), 513-527.https://doi.org/10.2307/2986142.

Baxter, M. J., Cool, H. E. M., Jackson, C. M., 2005. Further studies in the compositional variability of colourless Romano-British vessel glass. Archaeometry, 47(1), 47-68. https://doi.org/10.1111/j.1475-4754.2005.00187.x.

Beck, L., Lebon, M., Pichon, L., Menu, M., Chiotti, L., Nespoulet, R., Paillet, P., 2011. PIXE characterisation of prehistoric pigments from Abri Pataud (Dordogne, France). X-Ray Spectrometry, 40(3), 219-223. https://doi.org/10.1002/xrs.1321.

Beck, L., Salomon, H., Lahlil, S., Lebon, M., Odin, G. P., Coquinot, Y., Pichon, L., 2012. Non-destructive provenance differentiation of prehistoric pigments by external PIXE. Nuclear Instruments and Methods in Physics Research Section B: Beam Interactions with Materials and Atoms, 273, 173-177. https://doi.org/10.1016/j.nimb.2011.07.068.

Bernard, H. R., 2017. Research methods in anthropology: Qualitative and quantitative approaches. Rowman & Littlefield.

Bernatchez, J. A., 2008. Geochemical characterization of archaeological ochre at Nelson Bay Cave (Western Cape Province), South Africa. South African Archaeological Bulletin, 63(187), 3-11. https://search.informit.org/doi/10.3316/informit.485994972962238.

Blanca, M. J., Arnau, J., López-Montiel, D., Bono, R., Bendayan, R., 2013. Skewness and kurtosis in real data samples. Methodology. https://doi.org/10.1027/1614-2241/a000057

Buxeda i Garrigós, J., 2018. Compositional Data Analysis, in Varela et al. (Eds.), The Encyclopedia of Archaeological Sciences, Wiley Blackwell, Chichester, pp.1-5.

Cain, M. K., Zhang, Z., Yuan, K. H., 2017. Univariate and multivariate skewness and kurtosis for measuring nonnormality: Prevalence, influence and estimation. Behavior research methods, 49(5), 1716-1735. https://doi.org/10.3758/s13428-016-0814-1

Chalmin, E., Huntley, J., 2018. Characterizing rock art pigments. In : Bruno David; Ian J. McNiven (Eds). The Oxford Handbook of the Archaeology and Anthropology of Rock Art, Oxford Handbook, http://www.oxfordhandbooks.com/view/10.1093/oxfordhb/9780190607357.001.0001/oxfordhb-9780190607357-e-48, 2018,

Chalmin, E., Scmitt, B., Chanteraud, C,. Chassin de Kergommeaux, A., Soufi, F., Salomon, H., 2021, How to distinguish red coloring matter used in prehistoric time? The contribution of visible near-infrared diffuse reflectance spectroscopy, Color Res. Appl., 46(3), 653-673. https://doi.org/10.1002/col.22647.

Chanteraud, C., Chalmin, E., Lebon, M., Salomon, H., Jacq, K., Noûs, C., Delannoy, J.J., Monney, J., 2021. Contribution and limits of portable X-ray fluorescence for studying Palaeolithic rock art: a case study at the Points cave (Aigueze, Gard, France). J. Archaeol. Sci. Rep., 37, 102898. https://doi.org/10.1016/j.jasrep.2021.102898.

Chessel, D., Dufour, A. B., Thioulouse, J., 2004. The ade4 package-I-One-table methods. R news, 4(1), 5-10.

David, B., Clayton, E., Watchman, A., 1993. Initial results of PIXE analysis on northern Australian ochres. Australian Archaeology, *36*(1), 50-57

Dayet,L., 2012. Matériaux, transformations et fonctions de l'ocre au Middle Stone Age: le cas de Diepkloof Rock Shelter dans le contexte de l'Afrique australe, PhD Dissertation, Université de Bordeaux I, Bordeaux. https://tel.archives-ouvertes.fr/tel-00814875/.

Dayet, L., 2021. Invasive and Non-Invasive Analyses of Ochre and Iron-Based Pigment Raw Materials: A Methodological Perspective, Minerals, 11(2), 210. https://doi.org/10.3390/min11020210.

Dayet, L., Texier, P. J., Daniel, F., Porraz, G., 2013. Ochre resources from the middle stone age sequence of Diepkloof Rock Shelter, Western Cape, South Africa. Journal of Archaeological Science, 40(9), 3492-3505.https://doi.org/10.1016/j.jas.2013.01.025.

Dayet, L., Le Bourdonnec, F. X., Daniel, F., Porraz, G., Texier, P. J., 2016. Ochre provenance and procurement strategies during the middle stone age at Diepkloof Rock Shelter, South Africa. Archaeometry, 58(5), 807-829.https://doi.org/10.1111/arcm.12202.

Domingo, I., & Chieli, A., 2021. Characterizing the pigments and paints of prehistoric artists. Archaeological and Anthropological Sciences, 13(11), 1-20. https://doi.org/10.1007/s12520-021-01397-y

Eiselt B, Popelka-Filcoff RS, Darling A, Glascock M., 2011. Hematite sources and archaeological ochres from Hohokam and O'odham sites in Central Arizona: an experiment in type identification and characterization. *J Archaeol Sci* 38:3019–3028

Eiselt, B. S., Dudgeon, J., Darling, J. A., Paucar, E. N., Glascock, M. D., Woodson, M. K., 2019. In-situ sourcing of hematite paints on the surface of hohokam red-on-Buff ceramics using laser ablation–inductively coupled plasma–mass spectrometry (LA–ICP–MS) and instrumental neutron activation analysis. Archaeometry, 61(2), 423-441.https://doi.org/10.1111/arcm.12427.

Enserro, D. M., Demler, O. V., Pencina, M. J., D'Agostino Sr, R. B., 2019. Measures for evaluation of prognostic improvement under multivariate normality for nested and nonnested models. Statistics in medicine, 38(20), 3817-3831. https://doi.org/10.1002/sim.8204

d'Errico, F., 2003. The Invisible Frontier: A Multiple Species Model for the Origin of Behavioral Modernity, Evol. Anthropol. 12, 188–202. https://doi.org/10.1002/evan.10113.

Fernandes, P., Raynal, J.-P., Moncel, M.-H., 2008. Middle palaeolithic raw material gathering territories and human mobility in the southern massif central, france : first result from a petro-archaeological study on flint. *Journal of Archaeological Science*, 35(8), 2357–2370. https://doi.org/10.1016/j.jas.2008.02.012.

Glascock, M. D., Neff, H., Vaughn, K. J., 2004. Instrumental neutron activation analysis and multivariate statistics for pottery provenance. Hyperfine Interactions, 154(1), 95-105. https://doi.org/10.1023/B:HYPE.0000032025.37390.41.

Grave, P., Lisle, L., Maccheroni, M., 2005. Multivariate comparison of ICP-OES and PIXE/PIGE analysis of east Asian storage jars. *Journal of Archaeological Science*, 32(6), 885-896. https://doi.org/10.1016/j.jas.2005.01.011.

Green, R. L., Watling, R. J., 2007. Trace element fingerprinting of Australian ocher using laser ablation inductively coupled plasma-mass spectrometry (LA-ICP-MS) for the provenance establishment and authentication of indigenous art. Journal of forensic sciences, 52(4), 851-859. https://doi.org/10.1111/j.1556-4029.2007.00488.x.

Heginbotham, A., Bassett, J., Bourgarit, D., Eveleigh, C., Glinsman, L., Hook, D., Smith, D., Speakman, R. J., Shugar, A., Van Langh, R., 2015. The C opper CHARM S et: A New S et of Certified Reference Materials for the Standardization of Quantitative X-Ray Fluorescence Analysis of Heritage C opper Alloys. Archaeometry, 57(5), 856-868. https://doi.org/10.1111/arcm.12117

Hein, A., Tsolakidou, A., Iliopoulos, I., Mommsen, H., i Garrigós, J. B., Montana, G., Kilikoglou, V., 2002. Standardisation of elemental analytical techniques applied to provenance studies of archaeological ceramics: an inter laboratory calibration study. *Analyst*, 127(4), 542-553. https://doi.org/10.1039/B109603F.

Hodgskiss, T., 2010. Identifying Grinding, Scoring and Rubbing Use-Wear on Experimental Ochre Pieces. J. Archaeol. Sci. 37(12), 3344–3358. https://doi.org/10.1016/j.jas.2010.08.003.

Hodgskiss, T., 2014. The Cognitive Requirements for Ochre Use in the Middle Stone Age at Sibudu, South Africa. Camb. Archaeol. J. 24(3), 405–428. https://doi.org/10.1017/S0959774314000663.

Huntley, J., 2021. Australian Indigenous ochres: Use, sourcing, and exchange. The Oxford Handbook of the Archaeology of Indigenous Australia and New Guinea. Oxford: Oxford University Press. https://doi.org/10.1093/oxfordhb/9780190095611.013, 21.

Iriarte, E., Foyo, A., Sánchez, M. A., Tomillo, C., Setién, J., 2009. The origin and geochemical characterization of red ochres from the Tito Bustillo and Monte Castillo caves (northern Spain). Archaeometry, 51(2), 231-251.https://doi.org/10.1111/j.1475-4754.2008.00397.x.

Jercher, M., Pring, A., Jones, P. G., Raven, M. D., 1998. Rietveld X-ray diffraction and X-ray fluorescence analysis of Australian aboriginal ochres. Archaeometry, 40(2), 383-401. https://doi.org/10.1111/j.1475-4754.1998.tb00845.x.

Kasztovszky, Z., Maróti, B., Harsányi, I., Párkányi, D., Szilágyi, V., 2018. A comparative study of PGAA and portable XRF used for non-destructive provenancing archaeological obsidian. *Quaternary International*, 468, 179-189. https://doi.org/10.1016/j.quaint.2017.08.004.

Kiehn, A. V., Brook, G. A., Glascock, M. D., Dake, J. Z., Robbins, L. H., Campbell, A. C., Murphy, M. L. 2007. Fingerprinting specular hematite from mines in Botswana, Southern Africa, in: M.D Glascock, R.J. Speakman, R.S. Popelka-Filcoff (Eds.), Archaeological Chemistry: Analytical Techniques and Archaeological Interpretation, ACS Symposium Series 968, American Chemical Society, Washington DC, 2007, pp. 460-479.

Korkmaz, S., Goksuluk, D., Zararsiz, G., 2014. MVN: An R package for assessing multivariate normality. *The R Journal*, 6(2), 151-162.

Lebon, M., Beck, L., Grégoire, S., Chiotti, L., Nespoulet, R., Menu, M., Paillet, P., 2014. Prehistoric pigment characterisation of the Abri Pataud rock-shelter (Dordogne, France). Open journal of Archaeometry, 2(1). https://doi.org/10.4081/arc.2014.5456.

Lebon, M., Pichon, L., Beck, L., 2018. Enhanced identification of trace element fingerprint of prehistoric pigments by PIXE mapping. *Nuclear Instruments and Methods in Physics Research Section B: Beam Interactions with Materials and Atoms*, 417, 91–95. https://doi.org/10.1016/j.nimb.2017.10.010

Lebon, M., Gallet, N., Bondetti, M., Pont, S., Mauran, G., Walter, P., Bellot-Gurlet, L., Puaud, S., Zazzo, A., Forestier, H., Auetrakulvit, P., Zeitoun, V., 2019. Characterization of painting pigments and ochers associated to Hoabinhian archaeological context at the rock paintings site of Doi Pha Kan (Thailand), J. Archaeol. Sci. Rep., 26, 101855. https://doi.org/10.1016/j.jasrep.2019.05.020.

Leroy, S., 2010. *Circulation au moyen âge des matériaux ferreux issus des Pyrénées ariégoises et de la Lombardie. Apport du couplage des analyses en éléments traces et multivariés*. Doctoral Dissertation, Université de Technologie de Belfort-Montbeliard. https://tel.archives-ouvertes.fr/tel-00598796.

Leroy, S., Cohen, S., Verna, C., Gratuze, B., Téreygeol, F., Fluzin, P., Bertrand, L., Dillmann, P., 2012. The medieval iron market in Ariège (France).Multidisciplinary analytical approach and multivariate analyses. *J. Archaeolog. Sci*., 39(4), 1080–1093. https://doi.org/10.1016/j.jas.2011.11.025.

MacDonald, B. L., Hancock, R. G. V., Cannon, A., Pidruczny, A., 2011. Geochemical characterization of ochre from central coastal British Columbia, Canada. *Journal of Archaeological Science*, 38(12), 3620-3630.

MacDonald, B. L., Hancock, R. G. V., Cannon, A., McNeill, F., Reimer, R., Pidruczny, A., 2013. Elemental analysis of ochre outcrops in southern British Columbia, Canada. Archaeometry, 55(6), 1020-1033. https://doi.org/10.1111/j.1475-4754.2012.00719.x.

MacDonald, B. L., Fox, W., Dubreuil, L., Beddard, J., Pidruczny, A., 2018. Iron oxide geochemistry in the Great Lakes Region (North America): Implications for ochre provenance studies. Journal of Archaeological Science: Reports, 19, 476-490.https://doi.org/10.1016/j.jasrep.2018.02.040.

Maindonald, J., Braun, J., 2006. Data analysis and graphics using R: an example-based approach (Vol. 10). Cambridge University Press.

Martín-Fernández, J. A., Barceló-Vidal, C., Pawlowsky-Glahn, V., 2003. Dealing with zeros and missing values in compositional data sets using nonparametric imputation. Mathematical Geology, 35, 253–278.

Mathis, F., Bodu, P., Dubreuil, O., Salomon, H., 2014. PIXE identification of the provenance of ferruginous rocks used by Neanderthals, Nucl. Instrum. Meth. B.s. 331, 275-279. https://doi.org/10.1016/j.nimb.2013.11.028.

Mauran, G., 2019 *Apports méthodologiques à la caractérisation des matières colorantes: application à l'abri orné de Leopard Cave (Erongo, Namibie)*. PhD-Dissertation, Museum national d'Histoire naturelle, Paris. https://tel.archives-ouvertes.fr/tel-03020872

Mauran G., Lebon M., Lapauze O., Nankela M., Caron B., Détroit F., Pleurdeau D., Bahain J.J., 2020. Archaeological ochres of the rock art site of Leopard Cave (Erongo, Namibia): looking for Later Stone Age socio-cultural behaviours. *African Archaeological Review*, 37, 527-550. https://doi.org/10.1007/s10437-020-09394-7.

Mauran, G., Caron, B., Detroit, F., Nankela, A., Bahain, J. J. Pleurdeau, P., Lebon, M., 2021a. Data pretreatment and multivariate analyses for ochre sourcing: Application to Leopard Cave (Erongo, Namibia), J. Archaeol. Sci. Rep., 35, 102757. https://doi.org/10.1016/j.jasrep.2020.102757.

Mitchell, D., Grave, P., Maccheroni, M., Gelman, E., 2012. Geochemical characterisation of north Asian glazed stonewares: a comparative analysis of NAA, ICP-OES and non-destructive pXRF. *Journal of Archaeological Science*, 39(9), 2921-2933.. https://doi.org/10.1016/j.jas.2012.04.044.

Moyo, S. Mphuthi, D. Cukrowska, E.. Henshilwood, C. S., van Niekerk, K., Chimuka, L., 2016. Blombos cave: Middle Stone Age ochre differentiation through FTIR, ICP OES, ED XRF and XRD, Quat. Int., 404, 20-29. https://doi.org/10.1016/j.quaint.2015.09.041.

Nel, P., Lynch, P. A., Laird, J. S., Casey, H. M., Goodall, L. J., Ryan, C. G., & Sloggett, R. J., 2010. Elemental and mineralogical study of earth-based pigments using particle induced X-ray emission and X-ray diffraction. Nuclear Instruments and Methods in Physics Research Section A: Accelerators, Spectrometers, Detectors and Associated Equipment, 619(1-3), 306-310. https://doi.org/10.1016/j.nima.2009.12.003.

Onoratini, G., 1985. Diversité minérale et origine des matériaux colorants utilises dès le paléolithique supérieur en Provence, Bull. Mus. Hist. Nat. (Marseille). 45,7-114.

Palarea-Albaladejo, J., Martin-Fernandez, J. A., 2013. Values below detection limit in compositional chemical data. Analytica Chimica Acta, 764, 32–43.

Palarea-Albaladejo, J., Martín-Fernández, J. A., Buccianti, A., 2014. Compositional methods for estimating elemental concentrations below the limit of detection in practice using R. Journal of Geochemical Exploration, 141, 71–77.

Perlès, C., 1987. Les industries lithiques taillées de Franchthi (Argolide, Grèce) I, Présentation Générale et Industries Paléolithiques. Excavations at the Franchthi cave, Fascicle 3. Excavations at Franchthi Cave–Greece-. Indiana University Press. Bloomington. Indianapolis.

Pichon, L., Calligaro, T., Lemasson, Q., Moignard, B., Pacheco, C., 2015. Programs for visualization, handling and quantification of PIXE maps at the AGLAE facility. *Nuclear Instruments and Methods in Physics Research Section B: Beam Interactions with Materials and Atoms*, 363, 48-54. https://doi.org/10.1016/j.nimb.2015.08.086.

Pichon, L., Beck, L., Walter, P., Moignard, B., Guillou, T., 2010. A new mapping acquisition and processing system for simultaneous PIXE-RBS analysis with external beam. Nuclear Instruments and Methods in Physics Research Section B: Beam Interactions with Materials and Atoms, 268(11-12), 2028-2033.https://doi.org/10.1016/j.nimb.2010.02.124.

Pierce, D. E., Wright, P. J., Popelka-Filcoff, R. S., 2020. Seeing red: an analysis of archeological hematite in east central Missouri. Archaeological and Anthropological Sciences, 12(1), 1-20. https://doi.org/10.1007/s12520-019-00984-4.

Popelka-Filcoff, R. S., Robertson, J. D., Glascock, M. D., Descantes, C., 2007. Trace element characterization of ochre from geological sources. Journal of Radioanalytical and Nuclear Chemistry, 272(1), 17-27.https://doi.org/10.1007/s10967-006-6836-x

Popelka-Filcoff, R. S., Miksa, E. J., Robertson, J. D., Glascock, M. D., Wallace, H., 2008. Elemental analysis and characterization of ochre sources from Southern Arizona. Journal of archaeological science, 35(3), 752-762.https://doi.org/10.1016/j.jas.2007.05.018.

Popelka-Filcoff, R., C. Lenehan, M. Glascock, J. Bennett, A. Stopic, J. Quinton, A. Pring, K. Walshe, 2012. "Evaluation of relative comparator and k0-NAA for characterization of Aboriginal Australian ochre." Journal of Radioanalytical and Nuclear Chemistry 291(1): 19-24

Popelka-Filcoff, R. S., Zipkin, A. M., 2022. The archaeometry of ochre sensu lato: A review. Journal of Archaeological Science, 137, 105530. https://doi.org/10.1016/j.jas.2021.105530

Rifkin, R., 2015. Ethnographic and Experimental Perspectives on the Efficacy of Red Ochre as a Mosquito Repellent, S. Afr. Archaeol. Bull., 70, 64–75. www.jstor.org/stable/24643609.

Rifkin, R., Dayet, L., Queffelec, A., d'Errico, F., Summers, B., Lategan, M., 2015. Evaluating the Photoprotective Effects of Red Ochre on Human Skin by in Vivo SPF Assessment: Implications for Human Evolution, Adaptation and Dispersal, PLoS ONE, 10.9, e0136090. https://doi.org/10.1371/journal.pone.0136090.

Ripley, B., Venables, B., Bates, D. M., Hornik, K., Gebhardt, A., Firth, D., Ripley, M. B., 2013 Package 'mass'. *Cran R*, 538.

Salomon, H., Vignaud, C., Coquinot, Y., Beck, L., Stringer, C., Strivay, D., d'Errico, F., 2012. Selection and heating of colouring material in the Mousterian level of Es-Skhul (c. 100 000 years BP, Mount Carmel, Israel), Archaeometry. 54(4), 698–722. https://doi.org/10.1111/j.1475-4754.2011.00649.x.

Salomon, H., Goemaere, E., Billard, C., Dreesen, R., Bosquet, D., Hamon, C., Jadin, I., 2016. Analyse Critique du protocole de caractérisation des hématites oolithiquesmis en place dans le cadre du projet collectif de recherche sur L'origine des hématites oolithiques exploitées durant la Préhistoire récente entre l'Eifel (DE) et la Normandie (FR). *Anthropologica et Praehistorica*, 125/2014:225–246.

Salomon, H., Chanteraud, C., de Kergommeaux, A. C., Monney, J., Pradeau, J. V., Goemaere, É., Coquinot, Y, Chalmin, E., 2021. A geological collection and methodology for tracing the provenance of Palaeolithic colouring materials. Journal of lithic studies, 8(1), 38-p. https://doi.org/10.2218/jls.5540.

Scadding, R., Winton, V., Brown, V., 2015. An LA-ICP-MS trace element classification of ochres in the Weld Range environ, Mid West region, Western Australia, J. Archaeol. Sci., 54, 300-312. https://doi.org/10.1016/j.jas.2014.11.017.

Smith, M. A., Fankhauser, B., Jercher, M., 1998. The changing provenance of red ochre at Puritjarra rock shelter, Central Australia: Late Pleistocene to present. In Proceedings of the Prehistoric Society 64 : 275-292. Cambridge University Press.

Solé, V., Papillon, E., Cotte, M., Walter, P., Susini, J. 2007. A multiplatform code for the analysis of energy-dispersive X-ray fluorescence spectra. *Spectrochim. Acta, Part B*, 62(1):63–68. https://doi.org/10.1016/j.sab.2006.12.002.

Speakman, R. J., Little, N. C., Creel, D., Miller, M. R., Iñañez, J. G., 2011. Sourcing ceramics with portable XRF spectrometers? A comparison with INAA using Mimbres pottery from the American Southwest. Journal of archaeological science, 38(12), 3483-3496. https://doi.org/10.1016/j.jas.2011.08.011.

Speakman, R. J., Shackley, M. S., 2013. Silo science and portable XRF in archaeology: a response to Frahm. Journal of Archaeological Science, 40(2), 1435-1443. https://doi.org/10.1016/j.jas.2012.09.033.

Steenstra, E. S., Berndt, J., Klemme, S., van Westrenen, W., Heginbotham, A., Davies, G. R., 2021. Analysis of the CHARM Cu-alloy reference materials using excimer ns-LA-ICP-MS: Assessment of matrix effects and applicability to artefact provenancing. Archaeometry, 1– 16. https://doi.org/10.1111/arcm.12729

Swann, C. P., Fleming, S. J., 1990. Selective filtering in PIXE spectrometry. Nuclear Instruments and Methods in Physics Research Section B: Beam Interactions with Materials and Atoms, 49(1-4), 65-69. https://doi.org/10.1016/0168-583X(90)90217-I.

Tsolakidou, A.,, Kilikoglou, V.b,2002. Comparative analysis of ancient ceramics by neutron activation analysis, inductively coupled plasma–optical-emission spectrometry, inductively coupled plasma–mass spectrometry, and X-ray fluorescence. *Analytical and bioanalytical chemistry*, 374(3), 566-572. https://doi.org/10.1007/s00216-002-1444-2.

Vega, E., Leroy, S., Dillmann, P., Pagès, G., Hendrickson, M., Téreygeol, F., 2019. L'analyse chimique des déchets sidérurgiques sur le terrain par pXRF Un jeu d'échelle sous contraintes. in C. Benech, N. Cantin, M.-A. Languille, A. Mazuy, L. Robinet, A. Zazzo (Eds.), Instrumentation portable. Quels enjeux pour l'archéométrie?, Editions des Archives Contemporaines, Paris, pp.213-229

Velliky, E. C., MacDonald, B. L., Porr, M., Conard, N. J., 2021. First large-scale provenance study of pigments reveals new complex behavioural patterns during the Upper Palaeolithic of south-western Germany, Archaeometry, 63(1), 173-193. https://doi.org/10.1111/arcm.12611.

Wadley, L., 2005a. Ochre Crayons or Waste Products? Replications Compared with MSA 'Crayons' from Sibudu Cave, South Africa, Before Farming, 3, 1–12. https://doi.org/10.3828/bfarm.2005.3.1.

Wadley, L., 2005b. Putting Ochre to the Test: Replication Studies of Adhesives That May Have Been Used for Hafting Tools in the Middle Stone Age, J. Hum. Evol. 49, 587–601. https://doi.org/10.1016/j.jhevol.2005.06.007.Wei, T., Simko, V., Levy, M., Xie, Y., Jin, Y., Zemla, J., 2017. Package 'corrplot'. *Statistician*, 56, 316-324.

Weigand, P., Harbottle, G., Sayre, E. V., 1977. Chapter 2 - Turquoise sources and source analysis: Mesoamerica and the southwestern U.S.A. In : Earle, T.K., Ericson, J. (Eds.), Exchange Systems in Prehistory, Academic Press, 15-34, https://doi.org/10.1016/B978-0-12-227650-7.50008-0.

Wickham, H., 2011. ggplot2. *Wiley Interdisciplinary Reviews: Computational Statistics*, 3(2), 180-185.

Yellin, J., Perlman, I., Asaro, F., Michel, H. V., Mosier, D. F., 1978. Comparison of neutron activation analysis from the Lawrence Berkeley Laboratory and the Hebrew University. *Archaeometry*, 20(1), 95-100. https://doi.org/10.1111/j.1475-4754.1978.tb00219.x.

Zipkin, A. M., Ambrose, S. H., Hanchar, J. M., Piccoli, P. M., Brooks, A. S., & Anthony, E. Y., 2017. Elemental fingerprinting of Kenya Rift Valley ochre deposits for provenance studies of rock art and archaeological pigments. Quaternary International, 430, 42-59. https://doi.org/10.1016/j.quaint.2016.08.032.

Zipkin, A. M., Ambrose, S. H., Lundstrom, C. C., Bartov, G., Dwyer, A., Taylor, A. H., 2020. Red Earth, Green Glass, and Compositional Data: A New Procedure for Solid-State Elemental Characterization, Source Discrimination, and Provenience Analysis of Ochres. Journal of Archaeological Method and Theory, 27(4), 930-970.https://doi.org/10.1007/s10816-020-09448-9.